Long-Term Vulnerability Assessment and Adaptation Planning for the San Francisco Public Utilities Commission Water Enterprise

Technical Report 3: Urban Water Demand

Prepared for:
San Francisco Public Utilities Commission

Prepared by:
University of Massachusetts Amherst, Hydrosystems Research Group

May 2020

Summary

San Francisco Public Utilities Commission is interested in understanding the vulnerability of their system to climate change. The Hydrosystems Group at the University of Massachusetts is currently engaged in a Long Term Vulnerability Assessment to help SFPUC understand which future conditions cause the system to fail in meeting its level of service goals. A significant driver of operations for SFPUC is water demand. This report outlines analysis undertaken to develop scenarios of long-term urban water demand forecasts at the daily timestep. The results of this analysis, in combination with hydrological stream flow time series, will provide direct inputs for a stress test that will be conducted on an infrastructure system model of the SFPUC water system.

We conduct uncertainty and sensitivity analysis to establish a plausible range of demand scenarios to be used in the stress test of the regional water system. We apply quasi random sampling to independent variables to develop many thousands of realizations of future demand from 2010-2070. We use the results of this analysis to explore the sensitivity of the model to each of the input variables through linear regression and global sensitivity analysis. Finally, we employ the Patient Rule Induction Method (PRIM) to understand which conditions lead to very high values of demand.

Informed by the uncertainty and sensitivity analysis, we establish annual scenarios of total demand for all customers based on the projection provided by Brattle (2018). SFPUC's share of total demand is established using observed values from FY2012-13. Lastly, annual demand values are downscaled to daily timestep using temperature timeseries to reflect seasonal fluctuations in demand.

1. Introduction

Context and Purpose

San Francisco Public Utilities Corporation (SFPUC) and the Hydrosystems group at the University of Massachusetts Amherst are currently engaged in a long-term vulnerability assessment to understand what the impact of climate change, in combination with other factors, will be on the SFPUC Hetch Hetchy Regional Water System (RWS) over the next 50 years. In a workshop conducted at the outset of the project, key decision makers within SFPUC were asked to identify key sources of vulnerability that they consider could put the organization at risk of not achieving its level of service goals and rank them in terms of importance and degree of uncertainty (Figure 1-1). Water demand was identified as a source of vulnerability, a central driver of water system operations and a key uncertainty affecting future performance of the system.

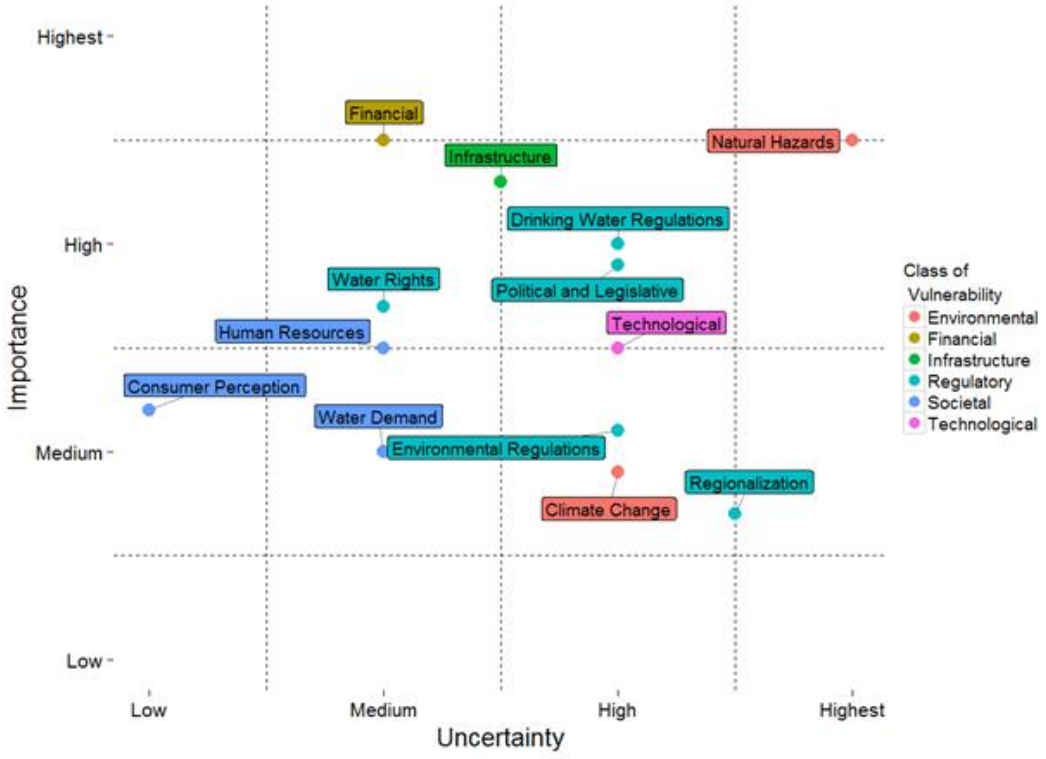

Figure 1-1: Importance and uncertainty associated with sources of vulnerability identified by SFPUC leadership .

The modeling framework used for the Long-Term Vulnerability Assessment (LTVA) is presented in Figure 1-2. The purpose of the demand module is to produce input time series of demand for the System Model (HRG TR4, 2021). The demand module converts plausible future annual demand scenarios to daily time series of demand of the wholesale customers, the in-City retail and some large suburban retail customers using temperature time series from the Weather Generator module HRG TR1 (2018).

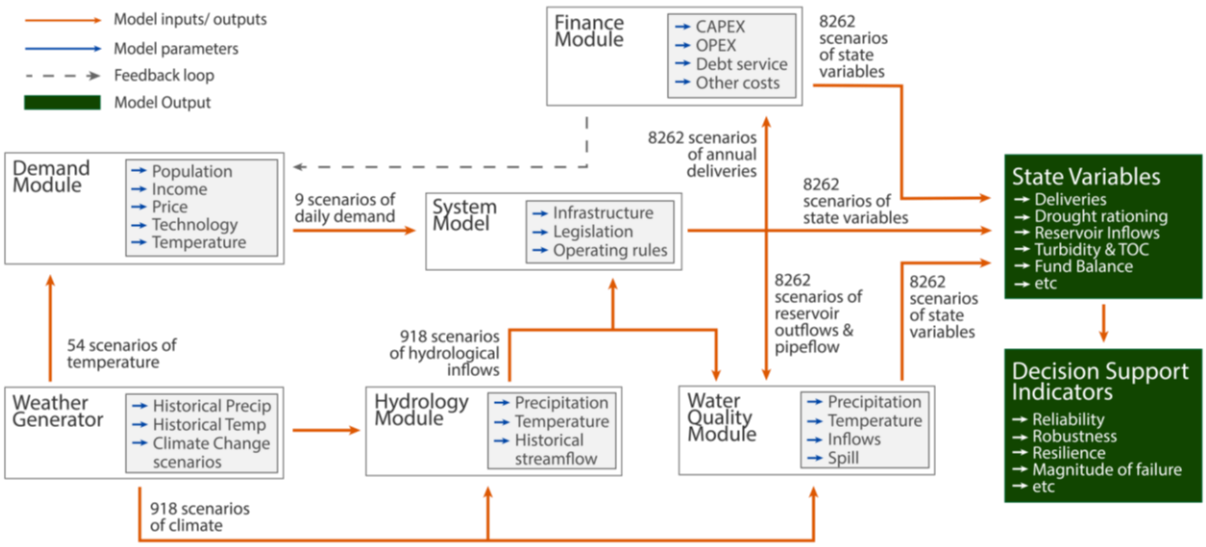

Figure 1-2: Schematic of the framework for the Long-Term Vulnerability Assessment

The purpose of this technical report is to document analyses conducted to develop scenarios and daily timeseries of water demand for use in the ongoing Long Term Vulnerability Assessment. Section One of this report provides a high level summary of the modelling approach and background on historical demand and existing projections in use by SFPUC. Section 2 describes baseline conditions used to initialize the model. Section 3 describes the uncertainty and sensitivity analysis conducted to establish the range of demand scenarios in 2070 whilst Section 4 describes these scenarios in relation to the Brattle (2018) projection. Section 5 documents the approach used to downscale annual demand to daily timeseries.

1.1. Modeling Approach

Currently, SFPUC water supply system planning model uses a single annual demand value disaggregated into three delivery centers with a fixed monthly pattern. The proposed demand module produces daily time series of demand for each customer. An illustration of the overall approach is provided in Figure 1-3. First, we explore the uncertainty of existing total demand projection model (section 3) to define scenarios of annual demand for the RWS (section 3.3) to be used in the LTVA stress test. The annual time series of demand for each customer are obtained starting with the baseline (section 2) and an adding and incremental amount a demand based on the work by the Brattle Group (Brattle, 2014, 18). We then establish the share of total demand that will fall to SFPUC based on the observed share of total demand from FY2012-2013. Lastly, we incorporate the influence of weather and climate through application of a heat function (section 5) and 9 synthetically generated sequences of temperature generated by the weather generator HRG TR1 (2018). These daily times series of demand for the RWS serve as input for the San Francisco Water System Model (SFWSM) (HRG TR4, 2021).

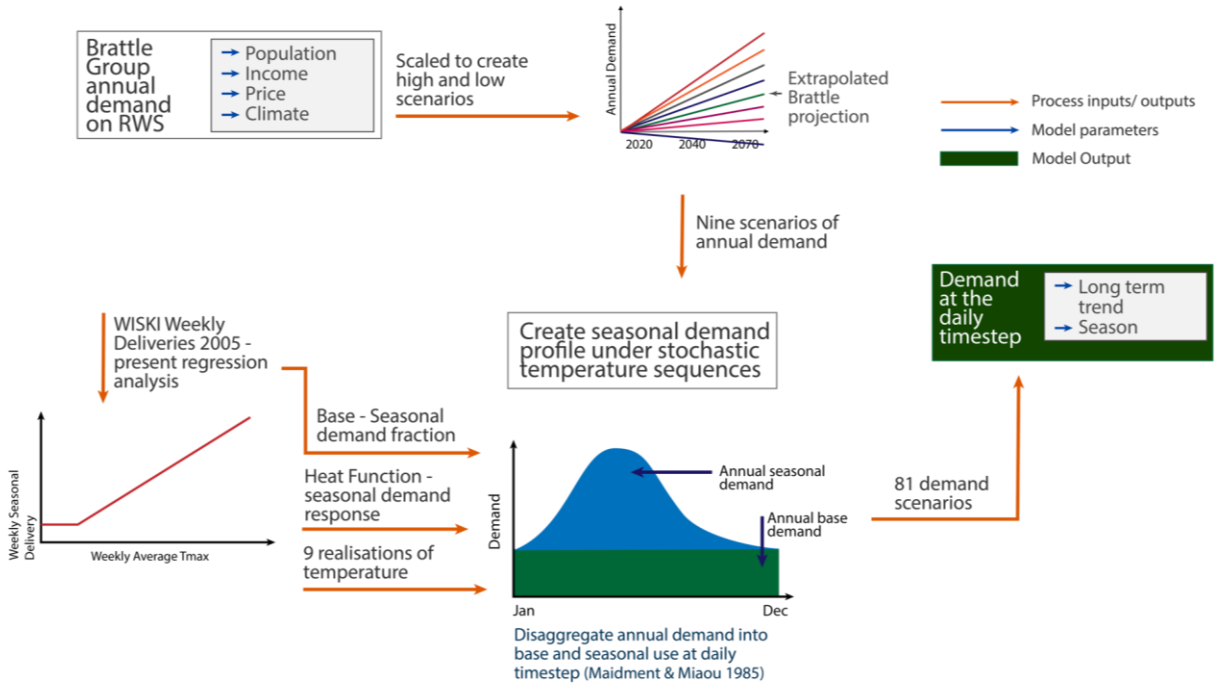

Figure 1-3: Schematic of demand module

1.2. Retail and wholesale customers

SFPUC provides water to both retail and wholesale customers. With the RWS, the SFPUC delivers water to 28 wholesale customers in Alameda, Santa Clara, and San Mateo Counties, including the Groveland Community Services District (Groveland CSD) in Tuolumne County (

Figure 1-5). Approximately two thirds of the SFPUC's water supply is delivered to wholesale customers, and the remaining one third is delivered to retail customers. The Bay Area Water Supply and Conservation Agency (BAWSCA) represents the interests of 26 of the wholesale customers and also coordinates their water conservation programming. The SFPUC also provides retail water service to customers in San Francisco and a small number of customers outside of San Francisco that are located along the RWS transmission system.

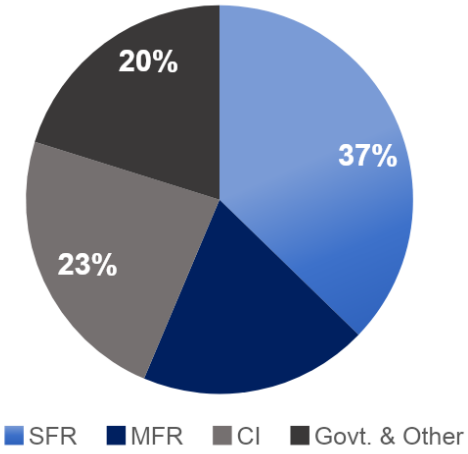

Figure 1-4: Breakdown of demand by sector in the SFPUC service area in 2010 (Brattle, 2018)

The SFPUC serves water for municipal and industrial users. As shown in Figure 1-4, residential demand (Single Family Residential (SFR) and Multi Family Residential (MFR)) makes up only about 50% of total demand. The other half of demand is made up of the commercial industrial sector and 'government & other'.

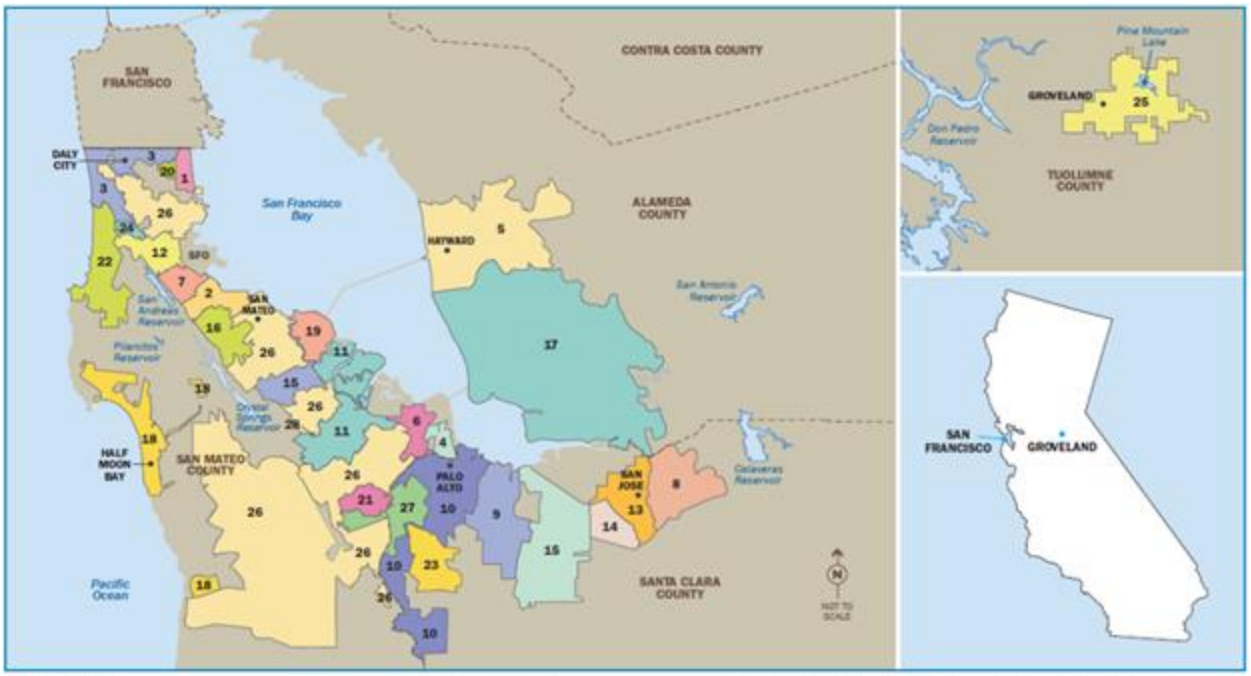

Figure 1-5: Map of SFPUC service area – the City of San Francisco and 28 wholesale customers (SFPUC, 2016).

Historical water usage across the SFPUC service area from 1972 through 2019 is presented in Figure 1-6. The times series shows the effects of droughts of 1976-77, 1987-92 and 2013-17 on the water consumption. Water conservation in the service area explains the steady decline since the early 2000s. The sharp decrease in water consumption from 2014 onwards is explained by the drought response throughout the service area. The consumption on the RWS does not represent the demand of the SFPUC

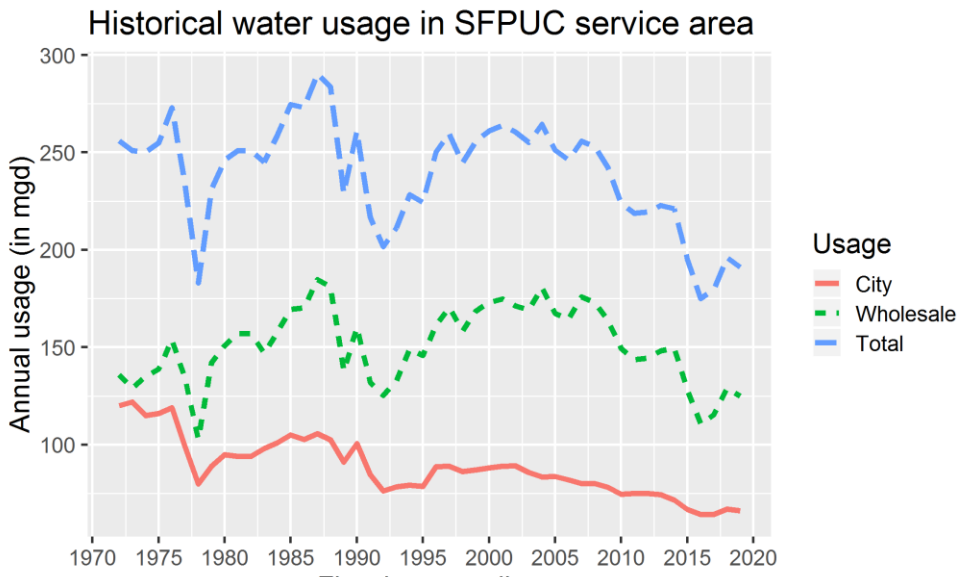

Figure 1-6: Historical water consumption on the RWS for the retail and wholesale customers from 1972 to 2019 (water usage data provided by SFPUC)

service area since several wholesale customers have other sources of supply. Since 1970, the SFPUC has supplied approximately 65% of total wholesale customers' demand. The dependence of each Wholesale customer on the RWS varies, with some entirely reliant on the SFPUC for their supply (Figure 1-7).

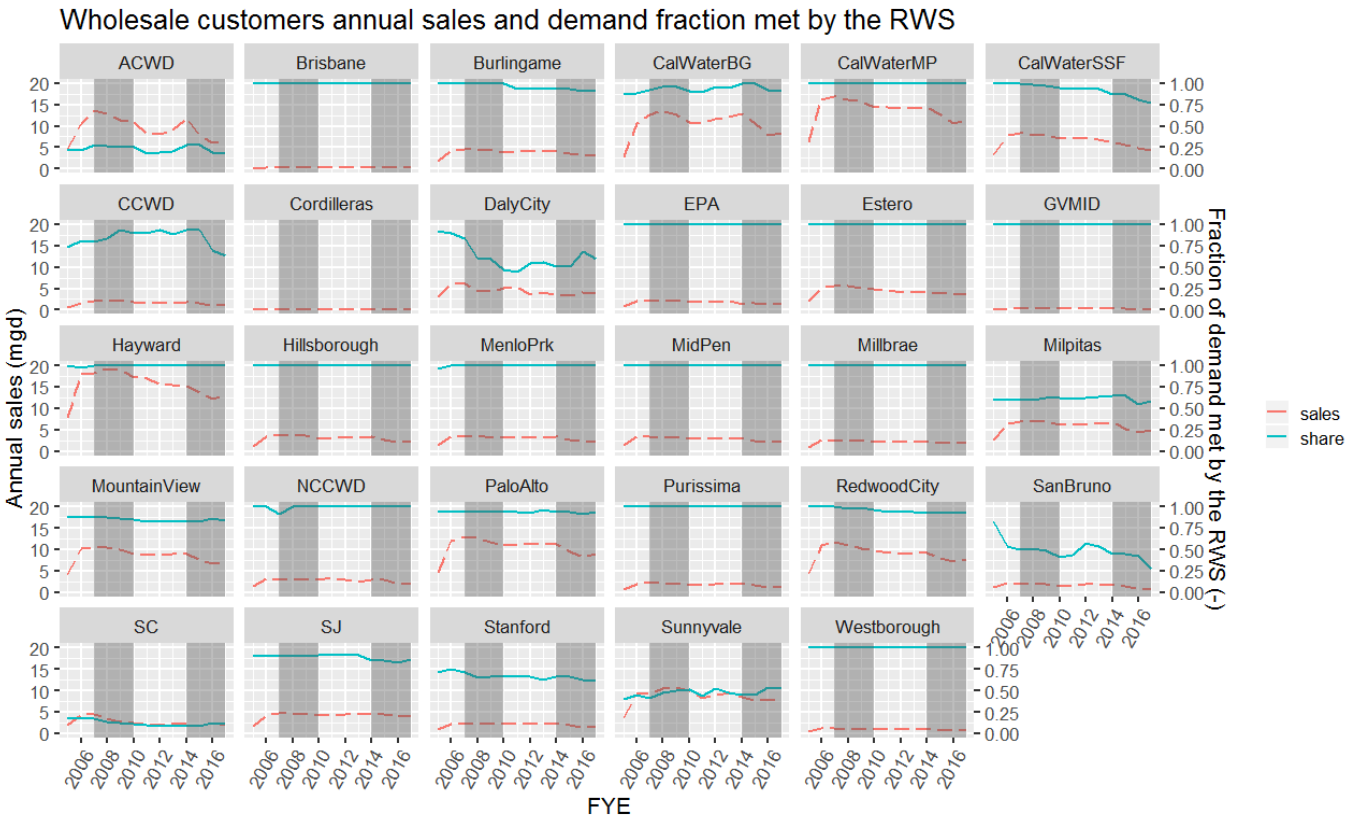

Figure 1-7: Wholesale customer demand and fraction of demand met by the RWS (share).

The wholesale water contractual obligations are outlined in the 2009 Wholesale Water Supply (WSA) Agreement (SFPUC, 2009). The WSA describes the "Supply Assurance" of 184 mgd for 24 of the 26 Wholesale Customers. The 184 mgd Supply Assurance is perpetual and survives the expiration of the WSA in 2034. The Supply Assurance includes the demands of the City of Hayward and 23 additional wholesale customers. The Supply Assurance is allocated between 23 wholesale customers using allocations called "Individual Supply Guarantees" (ISGs). The ISGs represent each customer's share of the Supply Assurance (Table 1-1). Separately, the City of Hayward has an unspecified supply allocation[1], included as the difference between 184 mgd and the sum of the customers' ISGs.

Customers with an ISG are referred to as permanent customers. Santa Clara and San Jose are not permanent customers and do not have ISGs in place but instead have Interim Supply Allocations (ISAs). The wholesale customers' collective allocation of 184 mgd includes the demands of the Cities of Hayward, San Jose, and Santa Clara.

[1] City of Hayward has an unspecified supply allocation due to the terms of a 1962 individual water supply contract with the SFPUC that did not contain a fixed allocation of water (SFPUC, 2016).

Table 1-1: breakdown of Individual Supply Guarantees (ISG) (share of Supply Assurance according to the 2009 WSA (SFPUC, 2009) for each wholesale customer

Wholesale Customer	ISG (mgd)	RWS Demand FY2012-13 (mgd)	Ratio between ISG and FY2013 demand
Alameda County Water District	13.76	9.06	0.66
Brisbane/GVMID	0.98	0.32	0.33
Burlingame	5.23	4.16	0.80
CWS - Bear Gulch	13.28	12.08	0.91
CWS - Mid Peninsula	14.66	14.04	0.96
CWS - South San Francisco	7.74	6.89	0.89
Coastside County Water District	2.18	1.67	0.77
Daly City	4.29	4.13	0.96
East Palo Alto Water District	3.46	2.08	0.60
Estero MID	5.90	4.05	0.69
Hayward	22.08	15.48	0.70
Hillsborough	4.09	3.25	0.79
Menlo Park	4.46	3.24	0.73
Mid-Peninsula	3.89	3.00	0.77
Millbrae	3.15	2.28	0.72
Milpitas	9.23	6.63	0.72
Mountain View	12.46	9.09	0.73
North Coast County Water District	3.84	2.51	0.65
Palo Alto	16.58	11.33	0.68
Purissima Hills Water District	1.63	1.99	1.23
Redwood City	10.93	9.31	0.85
San Bruno	3.25	2.01	0.62
Santa Clara	-	2.18	-
San Jose	-	4.50	-
Stanford University	3.03	2.14	0.70
City of Sunnyvale	12.58	9.54	0.76
Westborough Water District	1.32	0.91	0.69
Cordilleras MWC		0.01	

1.3. Existing Demand Projections

The Brattle Group (2014, 2015, 2018) prepared for SFPUC econometric models that incorporate weather and socio-economic factors to project urban water demand in the SFPUC service area through 2040. A summary of these various projections is provided in Figure 1-8 and the model is described in detail in section 3.1.1. For their report, individual specific water demand models were developed for the City of San Francisco and the Wholesale Customers. The demand models are based on separate models for the single-family residential (SFR), multi-family residential (MFR), and commercial and industrial (CI) sectors. The models were developed using historical data for estimating the relevant parameters. The initial conditions for the model represent normalized annual demand to remove the effects of unusual weather and economic conditions. The normalized base year demand for 2010 is estimated at 78 mgd for the City of San Francisco and 237 mgd for

the wholesale customers (Table 1-2) - total demand is 315 mgd. This is the represents the entirety of demand for customers and thus is greater than demand on the RWS.

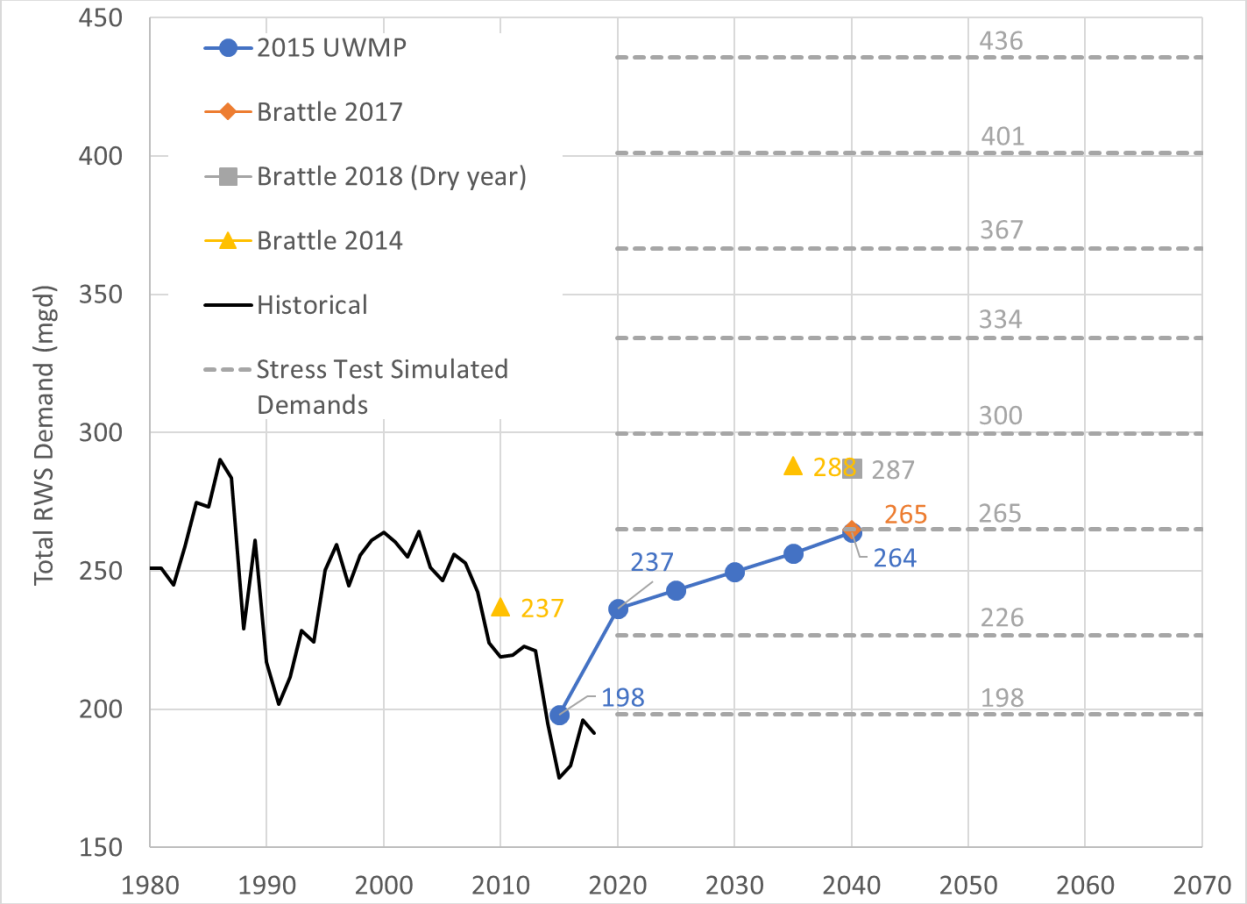

Figure 1-8 Historical demand on the RWS (black), projections of demand (colored symbols) and simulated demand scenarios for the stress test (dashed grey).

The demand projection starts with the base year and adds incremental amount of demand based on projected increases in population growth, employment, income, and the price of water, as well as the expected implementation of additional water conservation programs by San Francisco and the wholesale customers. Changes in income and price were coupled with estimations of consumer elasticities of demand to reflect the demand response of customers to these exogenous variables. The Association of Bay Area Governments (ABAG) projections developed in Plan Bay Area (https://www.planbayarea.org) were used to calculate expected growth rates for demand factors, except for price. Water price projections are generated based on SFPUC rate projections and the historical record of Wholesale Customer rates increases. The final step of the forecast process is a demand adjustment to account for the expected implementation of conservation programs by individual water agencies. The projected demand for the service area is generated by calculating SFR, MFR and CI water demands at the agency level and them summing demands across sectors and across agencies. Finally, 'Other' demands such as governmental uses, dedicated irrigation, unaccounted losses are added to the total. These values are taken from 2015 UWMP from customers (SFPUC, 2016).

For this study, the Brattle (2018) projection serves as the basis of our demand scenarios. The 2040 demand projections are estimated at 87.1 mgd for the City of San Francisco and 290.4 mgd for the wholesale customers (Table 1-2). The total demand is projected at 377.5 mgd.

Table 1-2: Summary of base year and year 2040 retail demands (Brattle, 2018)

	Base year	Year 2040
City of San Francisco	78	87.1
Wholesale customers	237	290.4
Total	315	377.5
Demand on RWS (dry year)	243	287
SFPUC share of total demand (fraction)	0.77	0.76

For SFPUC, an estimate of the demand on the RWS is needed for both the base year and year 2040, as opposed to total water demand. Considering the active water conservation and non-RWS supplies available to wholesale customers, The Brattle report (2018) estimates 2040 demand on the RWS during a dry-year to be 243 mgd and 287 mgd in a normal year (Table 1-2).

2. Baseline Demand

In order to evaluate the effects of drivers of change on the RWS, the system baseline has to be established. Demand on the system is an important component of this baseline. Baseline demand consists of both retail and wholesale demands. In consultation with SFPUC, it was decided to use pre-drought conditions of fiscal year (FY) 2012-2013 as the basis for baseline demand.

2.1. Retail Demand

Baseline values for retail demand are provided in Table 2-1 and are drawn from a mixture of sales in FY2012-13, the BEACON data deliveries, and values provided in SFPUC's 2015 Urban Water Management Plan (SFPUC, 2016). For the purpose of the system model, Cordilleras Mutual Water Company (MWC), a wholesale customer, was included in the retail demand. Demand for Cordilleras MWC is assumed constant over time.

Table 2-1: Baseline retail demand for the LTVA stress test analysis

Customer/ Region	Average Daily Demand (mgd)
In-City Retail	
Single Family Residential[1]	16.60
Multi-Family Residential[1]	22.60
Commercial and Industrial[1]	18.80
Other retail demand[2]	9.90
Water loss[3]	6.00
Total in-City	**73.9**
Suburban Retail	
Golden Gate Bridge Cemetery[4]	0.25
Menlo Park Country Club[4]	0.22

NASA[4]	0.62
San Francisco International Airport[4]	1.16
Town of Sunol[4]	0.58
Groveland CSD[4]	0.40
Lawrence and Livermore National Laboratories[4]	0.80
General Electric[4]	0.03
Other suburban retail[5]	0.92
Other[6]	0.01
Total suburban retail[6]	**5.00**
RETAIL TOTAL	**78.90**

1 Historical sales data for FY2012-13, which is used by SFPUC as a benchmark for 'normal' conditions prior to the 2013-17 drought.
2 This category includes other CI, institutional /governmental and landscape irrigation (both potable and non-potable). The estimates follow the same procedure as for the 2015 UWMP (SFPUC, 2016).
3 Water loss is assumed constant at 6 mgd and follows the procedure of the 2015 UWMP (SFPUC, 2016).
4 Sales data from SFPUC Customer Bureau. This value is an average and is assumed constant over time.
5 2015 UWMP provides a suburban retail demand total of 5 mgd. Other suburban retail represents the difference between this total demand value and the sum of suburban retail customers listed here.
6 Cordilleras MWC is a wholesale customer. For the purpose of the system model, it was added to the suburban retail demand with a constant demand of 0.01 mgd.

2.2. Wholesale Demand

Baseline values for the wholesale demand are provided in Table 2-2. The table shows annual sales for FY2012-13 and the fractions of the total demand that the sales represent. Total customer demand was established by dividing observed sales by the observed share of total demand. The fraction of demand met by the RWS varies from year to year for customers with multiple sources of supply, in particular in dry years. For this study, it was decided to keep this ratio constant and to set its value as that observed in FY 2012-2013.

Table 2-2: Baseline wholesale demand for the LTVA stress test analysis.

Wholesale Customer	Total Demand in FY2012-13[1] (mgd)	Demand on the RWS in FY2012-13[2] (mgd)	SFPUC share of Total Demand[3] (-)
Alameda County Water District	43.17	9.06	0.21
Brisbane/GVMID	0.32	0.32	1.00
Burlingame	4.48	4.16	0.93
CWS - Bear Gulch	12.71	12.08	0.95

CWS - Mid Peninsula	14.04	14.04	1.00
CWS - South San Francisco	7.41	6.89	0.93
Coastside County Water District	1.88	1.67	0.89
Daly City	7.38	4.13	0.56
East Palo Alto Water District	2.08	2.08	1.00
Estero MID	4.05	4.05	1.00
Hayward	15.48	15.48	1.00
Hillsborough	3.25	3.25	1.00
Menlo Park	3.24	3.24	1.00
Mid-Peninsula	3.00	3.00	1.00
Millbrae	2.30	2.28	0.99
Milpitas	10.21	6.63	0.65
Mountain View	10.83	9.09	0.84
North Coast County Water District	2.51	2.51	1.00
Palo Alto	11.80	11.33	0.96
Purissima Hills Water District	1.99	1.99	1.00
Redwood City	9.90	9.31	0.94
San Bruno	3.73	2.01	0.54
Santa Clara	21.77	2.18	0.10
San Jose	4.89	4.50	0.92
Stanford University	3.39	2.14	0.63
City of Sunnyvale	19.87	9.54	0.48
Westborough Water District	0.91	0.91	1.00
Cordilleras MWC	0.01	0.01	1.00

1 Estimated using the observed sales in FY2012-2013 (see reference below) and the observed RWS share of total demand.

2 Historical sales data for FY2012-13, which is used by SFPUC as a benchmark for 'normal' conditions prior to the 2013-17 drought.

3 Reference needed

3. Uncertainty and Sensitivity of Demand Projections

3.1. The case for uncertainty analysis

Demand forecasting is a fundamentally important exercise for water agencies in their long-term planning processes (Billing and Jones, 2011; Kiefer et al. 2016; Paton et al. 2013). How much demand will there be for water in the future? How much supply will be required to continue to

deliver a reliable service? How much will it cost to do so? and what are the financial implications for the consumer? In answering these questions, water agencies must attempt to predict how the future will manifest under a confluence of highly uncertain socio economic and climatic conditions. Getting it wrong can have significant economic, societal and environmental consequences. Overestimating poses the risk of over investment, stranded assets and high water rates, whilst underestimating can cause an increased risk of drought and water shortages. Forecasts of demand are rarely realized to a high degree of accuracy and have been spectacularly wrong in the past (Kiefer et al, 2016; Walker, 2012). Kielder Reservoir, the largest in the United Kingdom, was built in anticipation of significant employment and population growth that never materialized and today lies mostly idle (McCulloch, 2006).

Despite the central role of demand forecasting in any water utility planning exercise, and despite the substantial uncertainties associated with the key drivers of demand – population growth, economic growth, demographic change, climatic trends, land use change – surprisingly little attention has been paid to understanding the uncertainty associated with demand estimations, nor what the major drivers of that uncertainty are (Paton et al. 2013). In the face of this myriad of complex and interdependent drivers, a key question is - how wrong can you be? What is the plausible envelope of possible outcomes one can expect? and what are the drivers of that uncertainty?

Demand is typically evaluated in a deterministic fashion, using per capita consumption estimates or econometric models to produce point estimates of future demand (Billings and Jones, 2011; Fullerton and Molina, 2010; House-Peters and Chang, 2011; Kiefer et al., 2016; Rinaudo, 2013). Econometric approaches that estimate the response of customer classes to a variety of exogenous variables emerged in the 1980's, recognizing the importance of socioeconomic and climatic influences (Maidment et al. 1985; Maidment and Miaou, 1986), and are most common practice for large water utilities in the USA (Kiefer et al., 2013).

Water utilities most commonly plan for a single conception of what the future will look like. Those that do seek to explore uncertainty mostly do so by testing their plans against a handful of qualitatively derived scenarios that represent 'most likely' futures (Groves et al. 2015; Haasnoot et al., 2013; Kiefer et al. 2016). This approach assumes that decision makers can predict what the most likely future is, and which specific set of conditions will lead to its manifestation. Table 3 provides an overview of some notable examples of water demand and/or supply studies that have sought to address the uncertainty and sensitivity of their forecasts. Bureau of Reclamation (2012), Rayej et al. (2014), Groves et al. (2015), and Paton et al. (2013) all adopt a narrative based approach to define a small number of scenarios that provide a range of possible future demand. These studies, and many others, consider that population and employment growth will be the primary drivers of future 'high' and 'low' values of demand and as such, scenarios are largely expressed as variants in these parameters. Variations in income growth, price, nor elasticity values are explicitly explored. Hazen and Sawyer (2012) provide the only example we are aware of that takes a probabilistic approach to forecasting demand. In this case the probability distributions of socioeconomic and climatic variables were defined, and Monte Carlo simulation used to generate many realizations of demand and thus, confidence intervals around their central estimate. However, the analysis did not investigate which independent variables were the key drivers of this uncertainty, nor were elasticity of demand estimates included as uncertain variables. The range of demand forecasts in these studies is provided in Table 3 where available. Rayej et al. (2014) and Hazen & Sawyer (2012) are comparable at ~100%, whilst the range of scenarios used by the Bureau of Reclamation (2012) and Groves and Bloom (2013) was ~20%. Although conclusions are inferred regarding the sensitivity of the model across different demand scenarios, no quantitative approach is taken to measure model sensitivity as a distinct analytical step.

Decision making under deep uncertainty has emerged as an important field in recent decades, largely to support water managers in accounting for the significant uncertainty associated with climate change projections on hydrological systems. A growing body of literature provides well established mathematical models (Brown et al., 2012; Groves et al., 2015; Lempert et al., 2004; Weaver et al., 2013) that support the decision maker in identifying future conditions under which a policy fails to meet its goals (Walker et al. 2013; Hallegatte et al. 2012). These include approaches to generating many thousands of realizations of the future – through Latin Hyper Cube Sampling (McKay et al., 1979), Monte Carlo Simulation (Helton and Davis, 2003), and Sobol sequences (Saltelli, 2010; Sobol and Levitan, 1999) - for sensitivity analysis (Saltelli et al.1999, 2008, 2010; Sobol, 2001); and for scenario discovery (Bryant and Lempert, 2010; Friedman and Fisher, 1999; Groves and Lempert, 2007). To our knowledge these methodologies have not yet been applied to the question of long-term urban water demand forecasting.

Table 3-: Notable examples of water demand studies that have sought to account for uncertainty associated with demand forecasts.

Study Title	Location	Scope	Demand forecast methodology	Uncertainty Analysis Approach	Range of demand scenarios Increase in demand (% growth by 2070)	Sensitivity Analysis
Colorado River Basin Water Supply and Demand Study, **(Bureau of Reclamation, 2012; Groves and Bloom, 2013)**	Colorado, USA	Basin wide study across six States to develop 1959 scenarios of future streamflow, six demand scenarios and two reservoir operation scenarios.	Per Capita and unit area irrigation requirement estimates coupled with 6 scenarios of combinations of population, households, employment, irrigated land area and environmental IFR's.	Narrative based approach to develop six scenarios of low, medium, high demand based on of potential variations in population, employment, land use, irrigated crop area, environmental requirements, and conservation. These scenarios provide an envelope of demand projections. No account for price or income.	1.2 MAF to 5 MAF (5% to 24%) Population growth: 22.5% - 92.5%	No direct sensitivity analysis conducted. Differences in results across scenarios used to infer sensitivity of the model to input parameters. Found model to be most sensitive to population growth.
Scenarios of Future California Water Demand Through 2050, **(Rayej et al., 2014)**	California, USA	Statewide study to develop 108 scenarios to quantify future water demand for California.	Indoor demand and outdoor per capita water use derived from econometric model that incorporates elasticity factors accounting for income, price, family size and conservation and climate.	Narrative based approach to develop nine scenarios of population growth x development density and 12 scenarios of future climate. No account for income growth, price increase or elasticity uncertainty.	1 MAF to 7MAF (16% - 119%) Pop growth - 26% - 92% CI growth - 6% - 90%	No direct sensitivity analysis conducted. Differences in results across scenarios used to infer sensitivity of the model to input parameters. Found output to be most sensitive to population growth.
Developing Key Indicators for Adaptive Water Planning **(Groves et al. 2015)**	Southern California, USA	Application of RDM framework to Metropolitan Water District of California Service Area that developed 12 x climate, 26 x local supply yield, 3 x infrastructure upgrade and 4 x demand	Econometric model employing elasticities of demand for climate, household size, income, price, conservation and housing density explanatory variables.	A narrative based approach to develop four scenarios of demand based on demographic changes. Income growth rate remains constant across all scenarios. No account for income, price or elasticity uncertainty. Scenario discovery performed using PRIM analysis across results to establish conditions that lead to policy failure. Demand is determined to be a primary driver of vulnerability under 'high growth' scenario.	Unclear CI growth: 40% - 58% Income Growth: 36%	No direct sensitivity analysis conducted. Differences in results across scenarios used to infer sensitivity of the model to input parameters. Found output to be most sensitive to demand and infrastructure upgrade.

Relative magnitudes of sources of uncertainty in assessing climate change impacts on water supply security for the southern Adelaide water supply system **(Paton et al. 2013)**	Adelaide, Australia	Scenario based sensitivity analysis to establish the greatest drivers of uncertainty in security of supply estimates. Assessment of climate change impacts on Adelaide's water supply system.	Per capita indoor and outdoor consumption estimates for residential and commercial industrial sectors.	Narratives of potential socioeconomic and technological drivers of demand expressed in variants of per capita and population growth (median, 5th and 95th percentile of national forecast)	Unclear	Scenario based approach introduces uncertainty one by one from base case to qualitatively rank relative contributions of each uncertain parameter. Found demand to be the greatest source of uncertainty in all cases, ahead of climate change uncertainty.
Tampa Bay Water Probabilistic Demand Forecasting Procedure **(Hazen & Sawyer, 2012; Kiefer et al. 2016)**	Tampa Bay Florida, USA	Long-term water demand forecasting study to inform long term investment strategy for Tampa Bay Water	Probability distributions generated from historical observed changes to generate 'traces' of key model inputs (household income, housing density, and other socioeconomic variables) and empirically derived monthly distribution estimates for weather variables. Resulting distributions run through monte carlo simulations and run through econometric demand model.	Monte Carlo simulated realizations of future demand provide confidence intervals that are used by Tampa Bay Water to understand the possible envelope surrounding the mean demand projection.	15 MGD to 100 MGD (14% to 109%)	No sensitivity analysis conducted.

*The time scale considered varies from study to study. This 2070 takes the annual escalation estimated by the study and extrapolates to 2070 to facilitate comparison with analysis in this wor

1.2 Methods for Uncertainty Analysis

Analysis in this phase is focused on understanding the plausible envelope of uncertainty within which we can place SFPUC's existing 2040 projection of demand developed by the Brattle Group (2018). In addition, we are interested in exploring which parameters contribute most to this uncertainty. The intention is not to predict how the future might unfold nor establish the right answer with regards how much demand one should expect. Experiments are focused on characterizing the depth and nature of the uncertainty such that we develop a set of demand scenarios that capture the range of plausible future scenarios that SFPUC can expect by the year 2070. In addition, we seek to understand the drivers of this uncertainty – which parameters contribute most to the variance in the projection of demand? Are there certain parameters towards which we should focus our policy efforts in order to mitigate against the uncertainty they drive? And, are certain variables robust predictors of very high or very low values of demand?

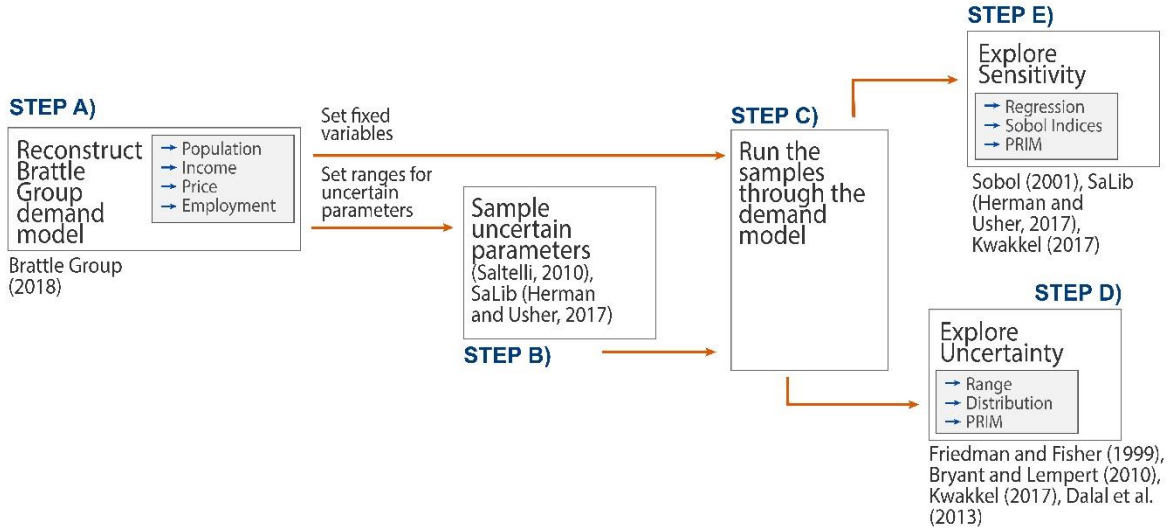

Figure 3-1: Schematic showing the approach taken for uncertainty and sensitivity analysis.

As a first step, we reconstruct the econometric model used by the Brattle Group (Brattle Group, 2018) to generate the demand forecast currently in use by SFPUC in its long term planning processes – Step A in Figure 3-1. Demand is calculated per sector as a function of population growth, economic growth, and of consumer response to changes in water price, median household income, precipitation and temperature. In order to establish the possible range of future demand and test the sensitivity of the model to its inputs (Step B), uncertain variables are sampled across defined distributions using Saltelli's (2010) extension of Sobol's sequence (Sobol, 1967) (Sobol's sequence is a quasi-random Monte Carlo method that ensures uniform sampling across the distribution of uncertain variables) to generate many thousands of plausible realizations of demand – Step C. In Step E, the sensitivity of the model to uncertain variables is first explored through linear regression and subsequently, through global sensitivity analysis provided by Sobol (2001).

The range and distribution of uncertainty associated with the model is explored through summary statistics and exceedance probability curves. The assumption of independence between uncertain variables is robust in this context due to ex-post examination of results in Step D. Scenario discovery, employing the Patient Rule Induction Method (PRIM), is used to establish which conditions lead to realizations of demand that would leave the SFPUC system vulnerable, i.e. at risk of not meeting its level of service goals. It is in this step where one can examine the likelihood that such conditions will materialize. We utilize pen source Python packages provided by Herman and Usher (2017), Kwakkel, (2017), and Hadka (2017) to execute various steps throughout the analysis.

3.1.1. Step A - Water demand model

Model structure and assumptions

In order to conduct uncertainty and sensitivity analysis on this model of demand, we first reconstructed the model used to generate the Brattle projection of demand. The demand model establishes demand of Single Family Residential (SFR), Multi-Family Residential (MFR) and Commercial Industrial (CI) customer classes for each of the 27 wholesale customers within the SFPUC service area at the annual timestep. The model schematic provided in Figure 3-1 illustrates how demand is calculated for each wholesale customer for a given timestep. It should be noted that the 'Government & Other' sector, which accounts for 20% of total demand across the SFPUC service area (see Figure 4) is not included in this analysis and thus the range of demand generated is likely to underestimate the uncertainty.

The governing equations for the demand model are provided in equations 1 through 3 where i denotes the customer class, t denotes the time step, q is the consumption per household or employee, ε^{i}_{k} is the elasticity of demand to variable k, $\%\Delta k$ is the annual escalation of variable k and %Δi is the annual escalation in the size of customer class i. Q^{i}_{t} is the total demand for customer class i in timestep t.

$$ln\left(q^{i}_{t}\right) = ln\left(q^{i}_{t-1}\right) + \left(\varepsilon^{i}_{pri} \times \%\Delta price\right) + \left(\varepsilon^{i}_{inc} \times \%\Delta inc\right) + \left(\varepsilon^{i}_{pcp} \times \%\Delta pcp\right) + \left(\varepsilon^{i}_{tmp} \times \%\Delta temp\right) \quad (1)$$

$$\#\ of\ i_t = \#\ of\ i_{t-1} \times \%\Delta i \quad (2)$$

$$Q^{i}_{t} = \#\ of\ i_{t} \times q^{i}_{t} \quad (3)$$

Equations 1 through 3 hold for all customer classes with a couple of adjustments. First, income and price elasticity for SFR households are calculated as a function of water price and median household income at each time step in the time series (equations 4 and 5). In the case of SFR, the regression coefficients for income ($\beta ln\ (inc)$), price ($\beta ln\ (pri)$) and the covariate coefficient of income vs price ($\beta ln\ (inc\ x\ pri)$) are inputs to the model and the calculation of price and income elasticity are intermediate outputs (see Figure 7) order to ensure these elasticities reflect consumer response to changes in real price and income, price and income values used in the derivation of elasticities are expressed in 2000 real terms[2], assuming an inflation rate of 2% per year (equations 6 and 7). Nominal Price and income for the year 2010 ($pri_{nom(2010)}, inc_{nom(2010)}$), the year in which the model is initialized, are provided as inputs to the model and the time period is denoted by n (n=11 in 2011, n=12 in 2012 etc).

[2] 2000 was the index year used by the Brattle group in the regression model used to derive consumer elasticities of demand (Brattle, 2015)

$$\varepsilon_{inc}^{SFR} = \beta\ ln\ (inc)\ +\ \beta\ ln\ (inc\ x\ pri)\ x\ ln(pri) \quad (4)$$

$$\varepsilon_{pri}^{SFR} = \beta ln\ (pri)\ +\ \beta ln\ (inc\ x\ pri)\ \ x\ ln(inc) \quad (5)$$

$$pri_{real(t)} = \frac{pri_{nom(2010)} \times (1 + (\%\Delta price\ \times n)}{(1 + interest\ rate)^{10+n}} \quad (6)$$

$$inc_{real(t)} = \frac{inc_{nom(2010)} \times (1 + (\%\Delta price\ \times n)}{(1 + interest\ rate)^{10+n}} \quad (7)$$

Second, only price, precipitation and temperature are considered as factors influencing demand for the Commercial Industrial (CI) sector.

The elasticities of demand used in this study are presented in Table 4 and are drawn from regression analysis conducted by the Brattle Group (Brattle, 2018) to establish the likely response of each customer class to various drivers of demand, based on observed behavior of customers from FY1996-97 through FY2010-11.

Due to the lack of available data associated with MFR accounts, analysts (Brattle, 2018) were unable to derive specific responses of this customer class to changes income, temperature or precipitation. In their reviews of income and price elasticities of demand for residential demand, Dalhuisen (2003) and Sebri (2014) found income elasticity to increase with increasing housing density, implying a more elastic response from MFR to increases in real median incomes. However, due to a lack of information, and because values of income elasticity for SFR are higher than considered in other regional studies (median of 0.966 across customers in 2010), MFR is assumed to have the same income elasticity as the SFR sector and remains fixed across all scenarios. MFR and SFR are assumed to have the same response to precipitation and temperature.

It should be noted that the Brattle Group (2018) did not include climate as a driver of demand (temperature and precipitation), nor did they include income as a driver of demand for the MFR sector. For the purposes of the uncertainty analysis temperature and precipitation (for all customer classes), and income (for SFR and MFR) were all included in the sampling and governing equations provided in equations 1-7.

How do elasticity estimates compare to other water demand studies?

In their study of future water demand for California, California Department of Water Resources (Rayej et al, 2014) used price elasticities of demand for SFR, MFR and CI of -0.16, -0.05 and -0.085 respectively and income elasticities of demand for SFR and MFR of 0.4 and 0.45 respectively. The results of the Brattle Group analysis across SFPUC service area would imply that its customers have a much more elastic response to both changes in price and income than is assumed in the California Water Department Study (SFR sector has a median price elasticity of -0.38 and median income elasticity of 0.97 in 2010 in the Brattle study).

Also, of particular relevance to this study is the Metropolitan Water District of California's study of water demand in Southern California (Groves et al., 2015) who used elasticities of demand for SFR, MFR and CI of -0.19, -0.16 and -0.16 respectively and income elasticities of demand for SFR and MFR of 0.27 and 0.31 respectively. Once again, the results of the Brattle Group analysis would imply that SFPUC customers have a much more elastic response to income and to price for SFR customers.

Table 3-1: Elasticities of demand per customer class. Elasticities represent the average demand response to a 1% increase in the demand factor. For example, a 10% increase in price would cause a -1.7% decrease in demand for Multi-family Residential and a 1.51% decrease in demand from the Commercial Industrial sector.

	Elasticity - average demand response to a 1% increase in the demand factor								
	Single Family Residential			**Multi-Family Residential**			**Commercial Industrial**		
	Elasticity	*95% conf interval*		**Elasticity**	*95% conf interval*		**Elasticity**	*95% conf interval*	
Price	-	-	-	-0.17	-0.26	-0.08	-0.151	-0.34	0.04
βln(pri)	-1.85	-2.21	-1.48	-	-	-	-	-	-
Median household income	-	-	-	-	-	-	-	-	-
βln(inc)	0.36	0.19	0.52	-	-	-	-	-	-
βln(incxpri)	0.56	0.42	0.70	-	-	-	-	-	-
Annual precipitation	-0.090	-0.13	-0.05	-	-	-	-0.04	-0.11	0.03
Average daily summer maximum temperature *	0.109	-0.08	0.3	-	-	-	0.482	-0.72	1.68

** for the purposes of this study we assume that a 1-degree increase in mean annual temperature will correspond to an equivalent increase in average daily maximum temperature.*

3.1.2. Step B - Quasi Random Sampling

Thoughtful consideration of meaningful distributions over which to sample independent variables is critical to the success of any sensitivity analysis (Saltelli, 2008; Saltelli, 2010; Ioos and Lemaître, 2015). This means establishing the range of uncertainty and distribution associated with each variable. In this study, we present two cases of analysis for which the results of analysis are presented:

- **Case 1: Regional Forecasts Uncertainty** considers the growth rates in exogenous drivers of demand (population growth, employment growth, price, income, temperature and precipitation) as its uncertain variables. In order to establish the range for growth in population, employment and income regional forecasts of population growth, demographic change and economic growth from different sources were examined and a 'high' and 'low' projection extracted to provide the bounds over which each variable is sampled. In the case of price, we used the range of projected price increase across all

wholesale customers established by the Brattle Group (2018). High and low scenarios of temperature and precipitation change were drawn from RAND (2019).

- **Case 2: Regional Forecasts and Elasticities Uncertainty** extends the analysis by also accounting for the uncertainty associated with the elasticity of demand estimate. These elasticities describe the demand response of customers to changes in the exogenous variables that are the focus of Case 1. As in any regression analysis, the regression coefficients established by Brattle (2018) have a 95th percentile confidence interval that describes the range of values within which one can be 95% confident that the true value of the parameter lies. For example, the regression coefficient for price, $\beta ln\,(pri)$, lies between -1.48 and -2.21. Over the course of the time horizon in question, a regression coefficient of -2.21 is likely to produce significantly different results than if a value of -1.48 is used. To account for this additional uncertainty, and to compare their relative contribution to the overall uncertainty, elasticities of demand are included in Case 2 as uncertain parameters and sampled across their 95th confidence interval values (see Table 4-1).

In this study we employ an extension of Sobol's sequence (Sobol and Levitan, 1999) provided by Saltelli (2010). Converse to Monte Carlo, and similarly to Latin Hyper Cube sampling, Sobol sequences are 'quasi random' – points 'know' about the position of previous point and fill the gaps between them to ensure that all parts of the sample space are represented (Saltelli, 2010).

The distributions of each of the uncertain parameters is provided in Table 3-2. The number of samples generated by the sampler is a function of the number of variables and is given by N x (2D + 2) where N is an input given by the analyst (often referred to as the computational cost) and D is the number of variables being sampled. This results in 18,000 samples for Case 1 (8 variables and N=1000) and 36,000 samples for Case 2 (16 variables and N=1000).

Table 3-2: Distribution of independent variables across cases considered in analysis

Parameter	**Abbreviation**	**Distribution of Values (p/a escalation)**	**Total Growth 2010-70 (range)**	**Comments**
Price	PRI_SFR	0.0223 to 0.0321	133.8% - 192.6% (58.8%)	Used range across wholesale customers in 2015 Urban Water Management Plans. Brattle (2018)
Income	INC	0.00958 to 0.0205	57.48% to 123% (65.52%)	ABAG (2009) forecasts a mean of 57% across wholesale customers CEF (2017) forecasts a mean of +123% by 2070 across Bay Area Counties

Conservation	CON	0.000 to 0.00820	0% - 49.2% (49.2%)	Used range across wholesale customers in 2015 Urban Water Management Plans. Brattle (2018)
Single Family Residential Growth	SFR	0.00343 to 0.00677	20.6% - 30.6% (10%)	2040 population forecasts: Low- Pitkin & Myers (2012) 2010-40 +25%; High - ABAG (2017): 2010-40 +33.2% (Housing projections are derived from population projections. The ABAG household projections utilize a population projection that is ~5% higher than those provided by Pitkin and Myers (2012))
Multi-Family Residential Growth	MFR	0.0108 to 0.0125	65.19% - 75% (10%)	
Commercial Industrial Growth	CI	0.00980 to 0.0153	58.8% - 92.0% (33.2%)	Low: mean across wholesale customers, +37.7% 2010-40 ABAG (2017); High: + 88% 2010-70 CEF (2017)
Temperature	TMP	0 to 0.00710		Representing 0 to 6 degrees Celsius warming and +/-30% change in precipitation, defined as most likely range by regional climate experts (RAND, 2019)
Precipitation	PCP	-0.00333 to 0.00333		

3.1.3. Step D - Scenario Discovery

The intention of scenario discovery is to identify whether combinations of uncertain model inputs are reasonable predictors of a model output (Bryant and Lempert, 2010). The hope is that, through this analysis, one can better understand which conditions might lead to policy failure. The approach provided by Bryant and Lempert employs the Patient Rule Induction Method (PRIM), a Bump Hunting algorithm (Friedman and Fisher, 1999) that slowly ('patiently') peels back layers of the output space to identify subspaces or 'boxes' that characterize samples of interest. Samples of interest are defined as model outputs that are above some defined threshold. In the context of this study, we investigate scenarios of demand that fall above the 75th percentile of all model outputs. This provides us with a large enough sample size for the algorithm to search within whilst also ensuring not all variables are included in the box definition – i.e. are constrained to some degree. In reality, demand above the 75th percentile is far beyond what SFPUC currently plans for and would be untenable for the existing system.

A box (B_k) is a hyper-rectangle that describes the intersection of subsets of values for each input variable. Let s_{jk} describe a subset of all possible values of input variable x_j and S_j denote all possible values of x_j. For the case in which the subset of values is the entire set, i.e. $s_{jk} = S_j$, the corresponding factor $x_j \in S_j$ can be omitted from the box definition. The input variables for which $s_{jk} \neq S_j$ are those that define the box (Friedman and Fisher, 1999):

$$x \in B_k \bigcap_{s_{jk} \neq s_j} (x_j \in s_{jk}) \quad (8)$$

Box induction occurs by first starting with a box that covers the entire dataset. With each iteration, a subbox of the previous is box is removed to produce the next, smaller box in the sequence. This iterative process of peeling back the sample space stops when the mean value of samples remaining in the subbox surpasses the target threshold. The boundaries of the resulting box are defined by the constrained values of the input variables.

In searching for boxes in the output space, PRIM seeks to maximize two measures of scenario quality; 1) coverage: the proportion of total cases of interest that are in the selected box, 2) density: the purity of the scenario space, i.e. the ratio of cases of interest to the total number of cases in that scenario. Coverage can be interpreted to mean the precision of positive predictive value (Dalal et al., 2013) whilst density is the overall predictive value, i.e. high density implies that the constrained variables that define a given box are highly predictive of model outcomes. The aim is to cover as many of the samples of interest as possible whilst containing as few as possible irrelevant samples (Kwakkel and Jaxa-Roxen, 2016). However, increases in one of these metrics is usually done so at the expense of the other (Kwakkel, 2017).

Box induction occurs recursively until all possible boxes have been defined. The result is a pareto front that trades off coverage and density metrics from which the analyst must decide which box they wish to examine in order to characterize samples that fall above the defined 'policy failure' threshold.

3.1.4. Step E - Sensitivity Analysis

Sensitivity analysis is concerned with understanding how uncertainty in the model output can be apportioned to the uncertainty associated with each of its input parameters and allows us to assert, for example, that this input "alone is responsible for 70% of the uncertainty in the output" (Saltelli, 2002; Saltelli, 2019). This understanding is useful in several ways:

- Identifying which factors contribute most to uncertainty in the model and thus warrant further investigation in order to reduce this uncertainty in the future.
- Identifying factors which interact and may propagate uncertainty.
- Model corroboration. Is the inference robust? Is the model overly dependent on fragile assumptions?

Many methods exist for sensitivity analysis but can be broadly characterized into two approaches; local sensitivity analysis (typically derivative based and considers the change in the model output when one variable is altered), and global sensitivity analysis that considers the entire variation range of inputs (typically evaluated using ANOVA). In this study, we employ both local sensitivity analysis (through linear regression) and global sensitivity analysis (through Sobol sensitivity indices).

Sobol sensitivity analysis (Sobol, 2001) is a variance-based approach that decomposes the variance in the model output according to its uncertain inputs. In their review of sensitivity analysis approaches, Ioos and Lemaitre (2015) provide a 'decision tree' for analysts in deciding which form of sensitivity analysis to employ. Sobol is recommended for nonlinear problems in which the

number of uncertain parameters is less than 20 and for which the model is not too computationally intensive. Sobol provides an advantage over other forms of sensitivity analysis in that it allows one to not only consider the individual contribution of each of the input parameters to the overall uncertainty, but also the contribution of multiple parameters in combination.

Sobol's first order index (S_i), provided by equations x, describes the relative importance of the uncertain variable X_i by considering the variance in the expected value of Y (the model output) given all possible values of X_i as a proportion of the total variance $V(Y)$:

$$S_i = \frac{V(E(X_i))}{V(Y)} \quad (9)$$

Sobol's total order index (S_{Ti}), provided by Equation 10, describes the total contribution of a variable to variance in the output, which includes both first order contributions as well as variance from the combination of the variable in question and any other model variables. The second term in Equation 10 describes the variance in the expected value of Y (the model output) given all terms but the variable question (X_{-i}). Given the sum of all possible sensitivity indices must equal 1, the difference must be made up of all terms that include X_i:

$$S_{Ti} = 1 - \frac{V(E(Y|X_{-i}))}{V(Y)} \quad (10)$$

3.2. Results

3.2.1. What is the range of uncertainty associated with a single model of demand?

The range of uncertainty varies considerably across the two cases presented here. Table 7 indicates the range in demand values in absolute terms and as a percent change relative to the 2010 baseline of ~281,000 AF/year. Whilst the range associated with Case 1 (27% - 183%) is comparable to those found by Hazen & Sawyer (2012) (14% - 109%), and Rayej at al. (2014) (16% - 119%), the range for Case 2, in which elasticity of demand uncertainties are included, result in ranges three to four times larger than any examples found in the literature. In addition, Case 2 shows a decrease in demand in the lower ranges, which is an outcome we have not come across in anywhere in the literature. The red dotted lines displayed in Figure 8 and Figure 9 show where the existing SFPUC demand projection in 2040 sits relative to the distributions of the two cases presented here.

Table 3-3: Change in demand by 2070 relative to 2010 baseline of 281 TAF/year

	Minimum		**Median**		**Maximum**	
	(AF)	% increase	(AF)	% increase	(AF)	% increase
Case 1: Regional Forecasts	356,191	27%	538,636	91%	796, 514	183%
Case 2: Regional Forecasts and elasticity uncertainty	265,383	-6%	563,575	101%	1,458,051	419%

Demand is not normally distributed given the exponential nature of the governing equation of demand provided in Equation 1. The box plots and exceedance probability curves in Figure 8 and Figure 9 indicate a lognormal distribution, with a large tail towards higher values of demand. However, a formal statistical test would need to be conducted to confirm this. This tail is most pronounced in Case 2, when the uncertainty associated with elasticity estimates is included.

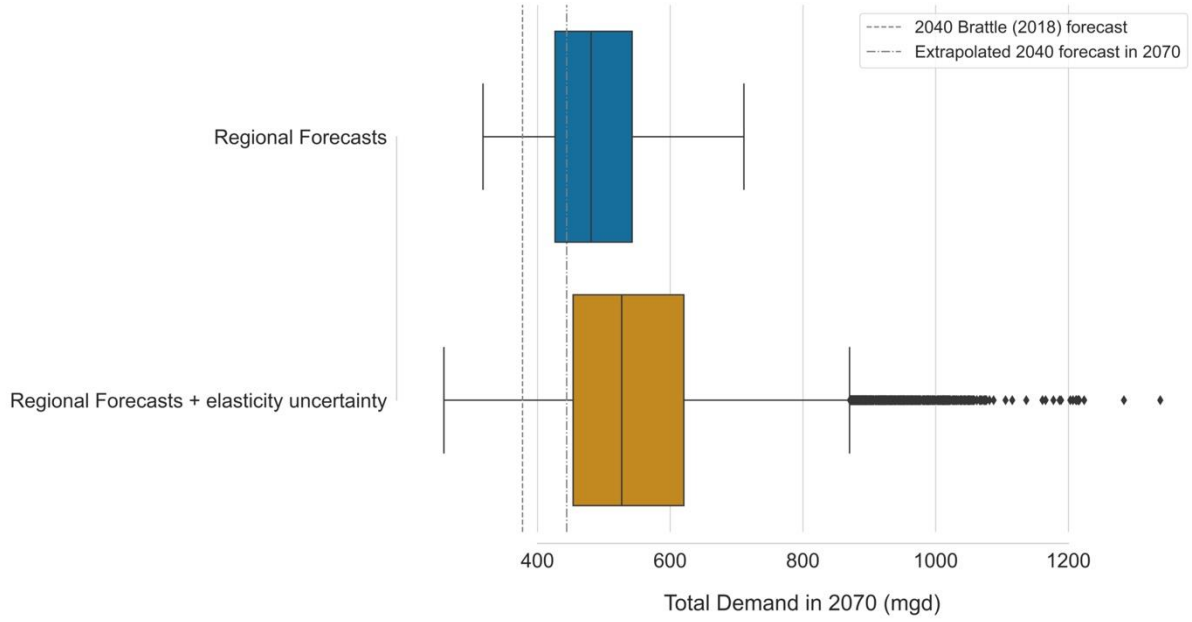

Figure 3-2: Box plot showing distribution of demand realizations for Case 1 (blue) and Case 2 (orange)

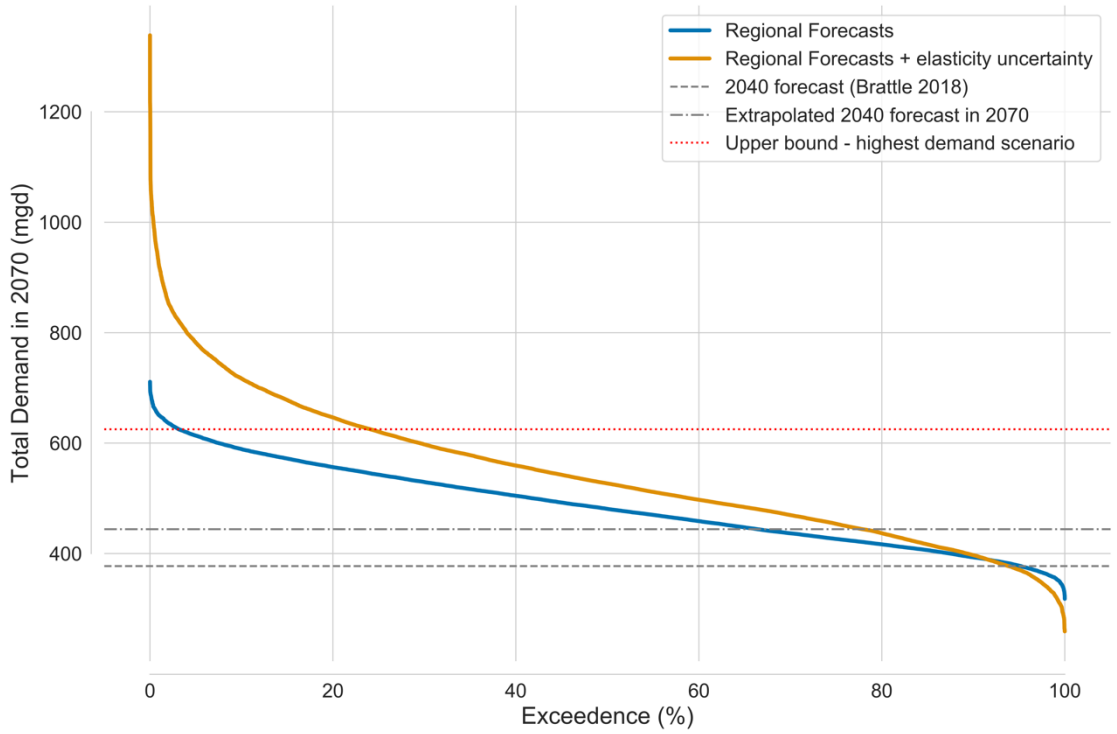

Figure 3-3: Exceedance probability curves of demand for Case 1 (blue) and Case 2 (orange). The Brattle forecast of demand in 2040 is indicated by the dashed grey line, the extrapolated Brattle forecast in 2070 is provided by the grey dash-dot line and the upper bound for demand scenarios presented here is provided by the dotted red line.

3.2.2. What conditions lead to 'unacceptably' high values of demand?

The density versus coverage trade off curves resulting from the application of PRIM to both Cases is presented in Figure 3-4. The points on the trade-off curves represent different sub spaces of the sample space of interest, whilst the values on the x and y axis provide their values of coverage and density respectively. The trade of curve for Case 1 provides relatively good metrics of coverage and density as can be seen from the convex nature of its trade off curve. Results from Case 2 are not as promising, showing a shallow, linear trade off curve that does not offer good options for boxes with both a high coverage and high density score. In addition, the number of constrained variables in each box (denoted through the color scale shown to the right of the plots) quickly increases to more than four variables for boxes with high density scores. This indicates a more complex picture than Case 1 with regards to which variables are accurate predictors of high demand – it is several factors in combination that result in high demand and there are many other conditions that also lead to high demand, indicated by the high proportion of samples of interest outside the box (coverage).

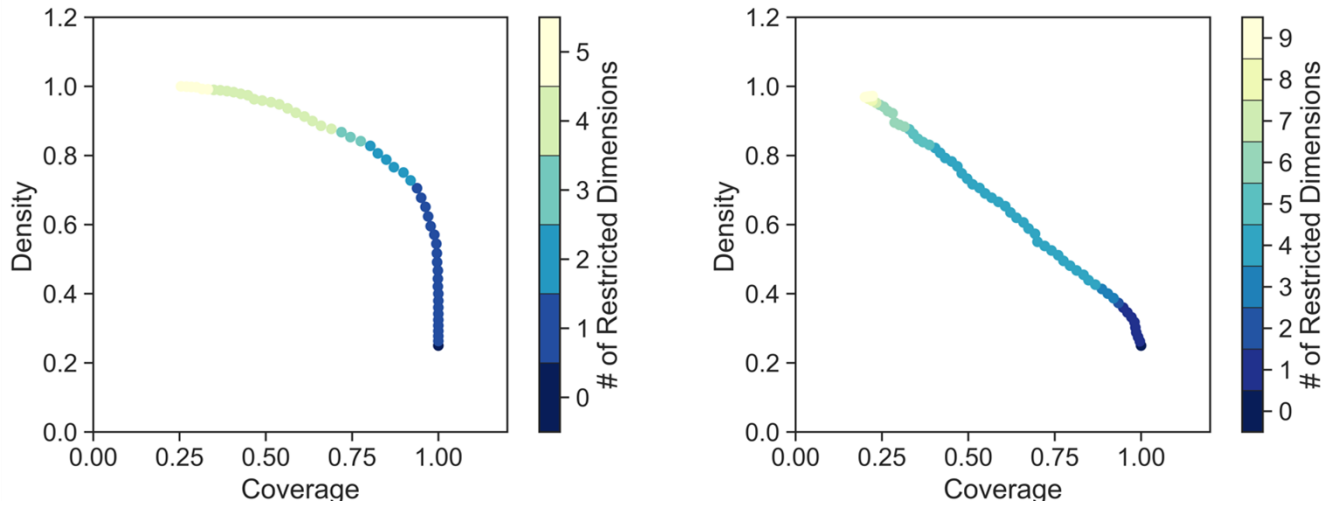

Figure 3-4: Density vs coverage tradeoff for Cases 1 (left) and 2 (right). Dots on the pareto front represent different Boxes found by the algorithm. The color of the dot indicates the number of input variables that are constrained according to the color scale to the right of the plot.

The box selected for Case 1 has a score of 80% for both coverage and density and thus provides reasonable predictive accuracy in establishing which conditions are likely to lead to high values of demand. The box coverage plot for this box is provided in Figure 3-5. Blue dots represent samples in the output space that fall below the defined 'policy failure' threshold, whilst red dots represent output samples of interest, i.e. those that result in demand higher than the 75% percentile of all model outputs. This provides us with a large enough sample size for the algorithm to search within whilst also ensuring not all variables are included in the box definition – i.e. are constrained to some degree. Visual inspection of the box (shown by the solid black line) confirms the high score for coverage and density: the majority of the samples of interest fall within the box (coverage) and most of the samples within the box are those of interest (density). Only two variables are shown to be constrained in this box: growth in income and price. Although price appears in the box definition, its values are constrained to growth of between 133.8% and 192%, which is almost the entire range over which this variable was sampled. Only price growth in the top 0.6% of its distribution are not represented in this box. This tells us that almost all values of price growth lead to these very high values of demand – only those samples in which price growth is between 192% growth and 192.6% growth by 2070 fall below the 75% percentile in terms of total demand in 2070. Income on the other hand is significantly constrained: only income growth of between 108% and 123% lead to values of demand that fall in the highest 25% of all model runs. This represents only the top 23% of the distribution over which income growth was sampled and indicates that high income growth is highly predictive of high demand under this model. It is worth pausing to remember the important role that income plays in driving the price elasticity of demand for single family residential households. Recall from Equation 5 that the price elasticity of demand for single family residential households is driven by the regression coefficient of price, the covariate regression coefficient of price times income and real income in the given timestep. Under conditions of high-income growth, the response of consumers to price is less elastic, i.e. less negative, leading to high demand even under conditions of high price growth.

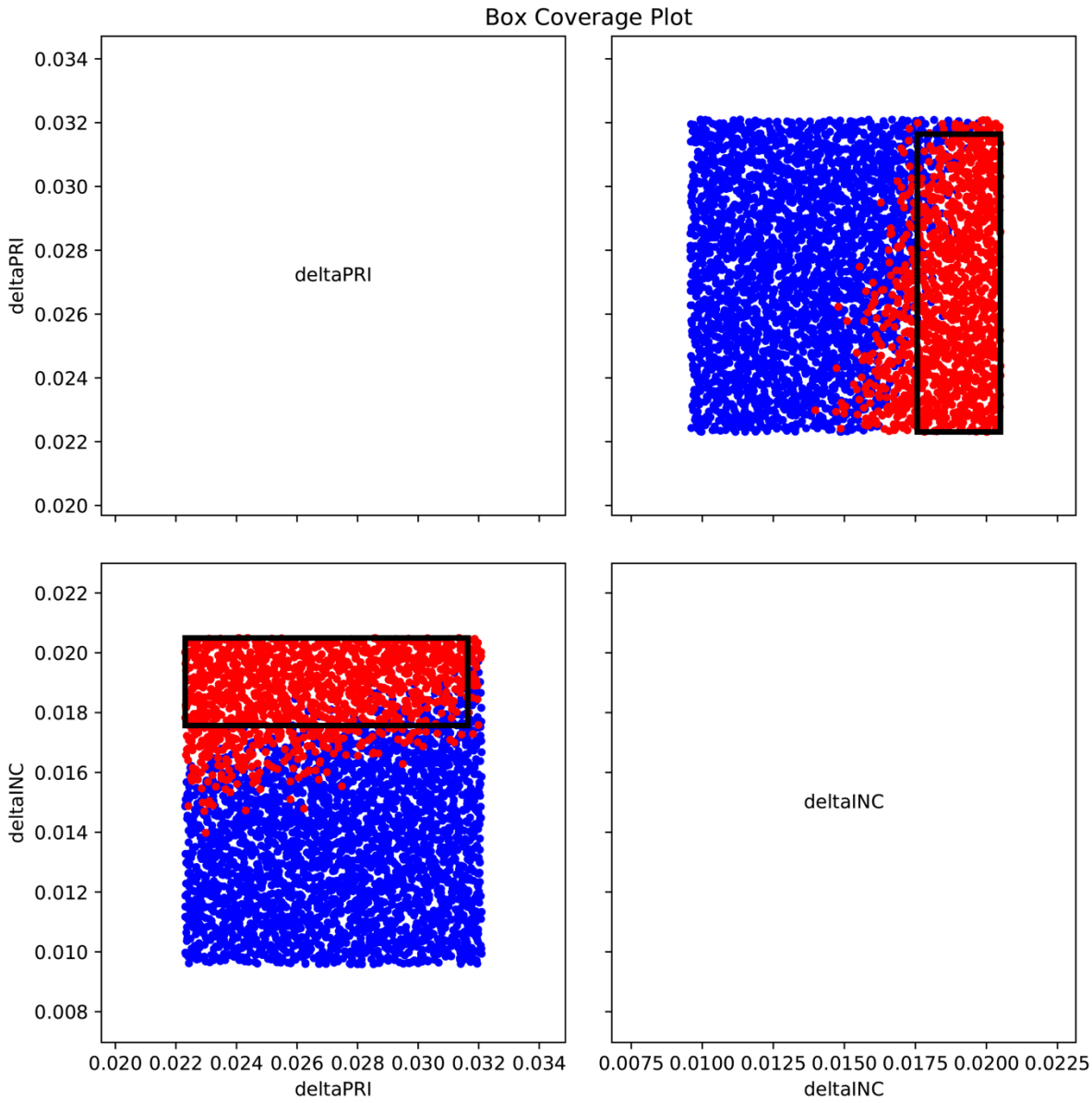

Figure 3-5: Box Coverage plot for Case 1. Red dots indicate samples of interest (those in which demand in 2070 is above the 75th percentile of all model outputs), blue dots are samples not of interest and the black solid line indicates the chosen Box. The degree to which input variables are constrained can be examined by considering the position of the box against the axis for each input variable.

When considering the box coverage plots for Case 2 (see Figure 3-6), a box with a score of 60% for density and coverage was chosen. Income growth is once again constrained to the higher end of its distribution (although less so than in the instance of Case 1) with growth restricted to between 90% and 123% growth by 2070, representing the top 50th percentile of its distribution. In this Case, the regression coefficients for price and the covariate of income x price for SFR are also found to be constrained to the higher end of their distribution (the top ~50th percentile for the covariate coefficient of price x income and the top ~75th percentile for the regression coefficient of price). The presence of the covariate of price x income in the box definition provides further evidence of

the important role that income and price elasticity plays in driving demand under this model. Recall from Equation 4 and 5 that income and price elasticity of demand for single family residential households is driven by the covariate coefficient of price x income. The presence of the regression coefficient for price for single family residential households points additionally to the role of price elasticity in driving high values of demand.

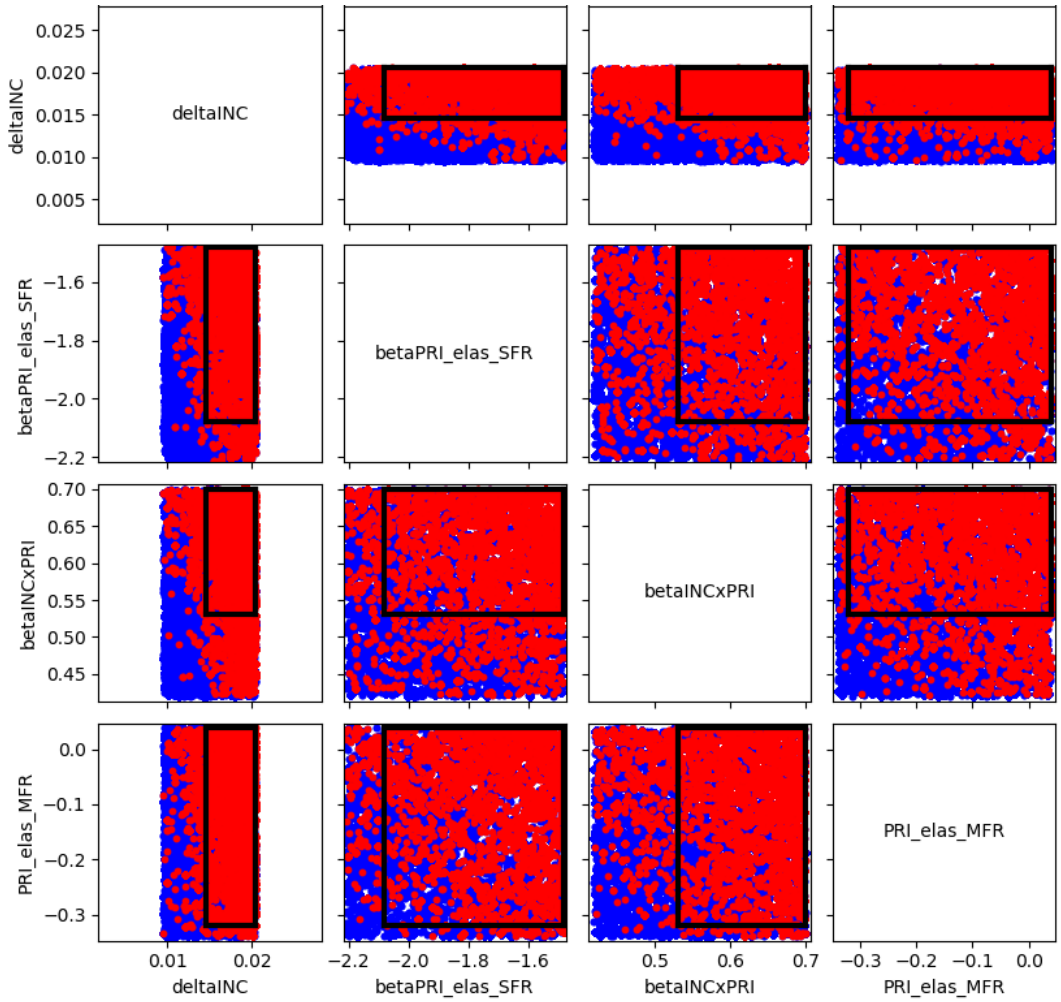

Figure 3-6: Box Coverage plot for the Case 2. Red dots indicate samples of interest (those in which demand in 2070 is above the 75th percentile of all model outputs), blue dots are samples not of interest and the black solid line indicates the chosen Box. The degree to which input variables are constrained can be examined by considering the position of the box against the axis for each input variable.

3.2.3. Which input parameters is the estimation of demand most sensitive to?

The figure shows the bivariate distributions of total demand, the output of the model, against each of the independent variables. The first column in the facet grid shows the results for Case 1 whilst the second and third columns show results for Case 2. Each column in the facet grid represents one of the four cases under consideration, and each row shows the results for a different independent variable. The data are displayed as joint histograms, where the color of the hexagonal bins indicate the number of data points that fall within the bin. The darker the blue, the higher the

density of data points. The histograms along the x axis indicate that, as expected, sampling of independent variables is uniform across their distributions. The same lognormal distribution of demand observed in the box plots and exceedance probability curves displayed in Figure 3-2 and Figure 3-3 can be seen in the histograms along the y axis. Not all regressions are provided here to facilitate interpretability. Only those variables that show a square of Pearson's correlation coefficient (R^2) value of greater than 0.01 are displayed. The exception is for growth in single family residential and multi-family residential households, which have been included given the prominence of population growth as a driver of demand in most demand studies in the literature. For both Case 1 and Case 2 the R^2 value for and residential (MFR and SFR) temperature and precipitation elasticities are less than 0.01.

A significant point of interest in considering these linear regression plots is that, besides income growth, the majority of input parameters show very little trend, with R^2 values of less than 0.1 for almost all variables across both cases. One can see by observing the spread of data points that for every value of most variables, there are demand values from across the entire distribution. This is interesting when considering typical approaches to establishing scenarios of demand that we have discussed here – high population and employment growth do not necessarily lead to high values of demand. Income growth shows the strongest signal in both Cases, showing a clear positive relationship with values of demand, and is strongest when elasticity coefficients are not included in the sensitivity analysis. For Case 1, price shows the strongest signal after income growth with a relatively clear relationship with demand - as expected, demand decreases with increasing price. For Case 2, where elasticity uncertainty is accounted for, the regression coefficients for price and income show the strongest signal after income growth, both with a 0.15 R^2.

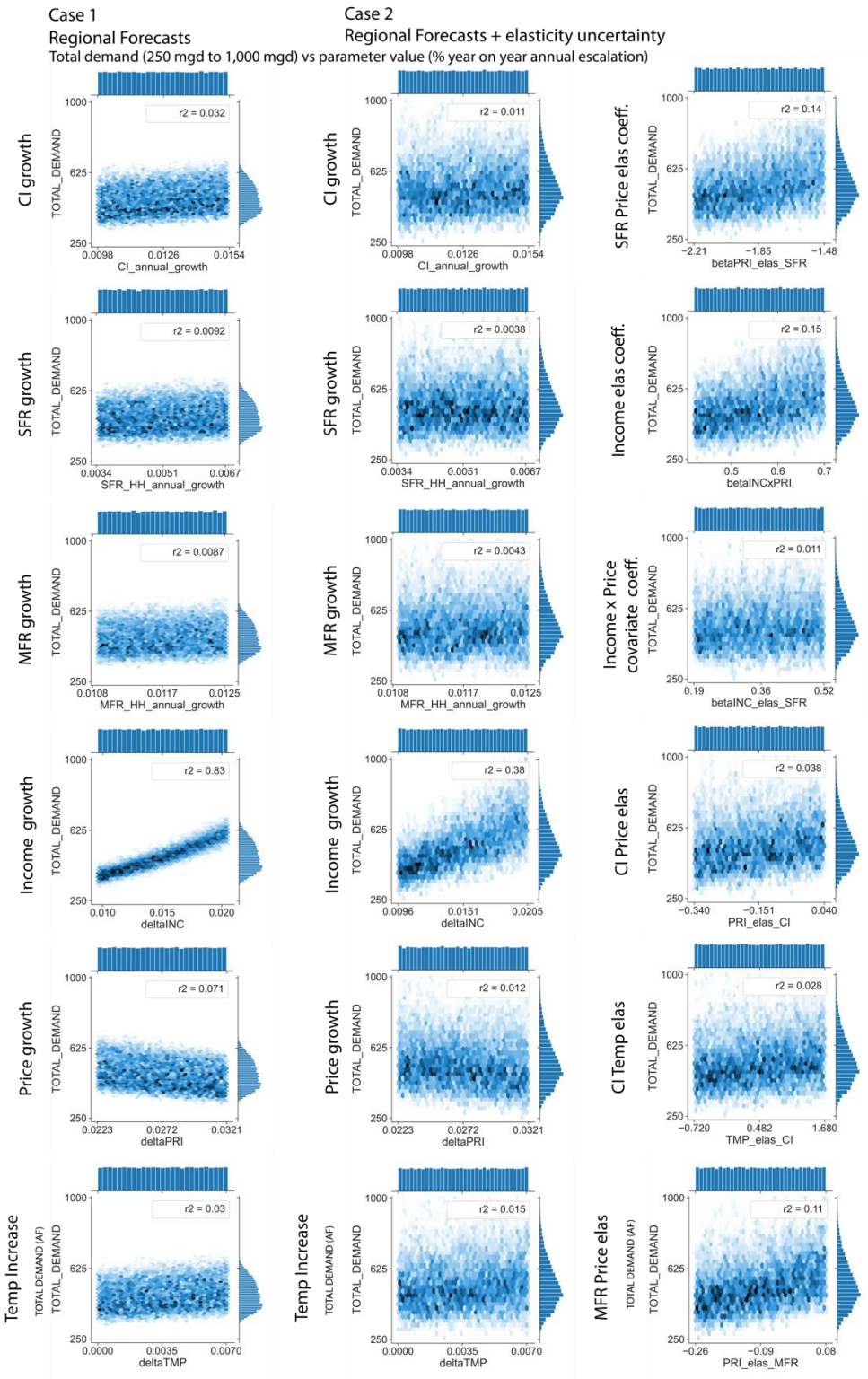

Figure 3-7: Scatter plots showing total demand in 2070 vs the predictors of demand subject to sampling and sensitivity analysis

Figure 3-8 shows the results of the Sobol sensitivity analysis. Only those variables that contribute more than 1.5% of the uncertainty in any of the Cases is included in the figure. Changes in precipitation, conservation, CI temperature and precipitation elasticities, residential (MFR and SFR) temperature and precipitation elasticities and the regression coefficient for income elasticity all contribute less than 1.5% of the total uncertainty.

In line with what is observed through linear regression, income growth drives uncertainty in the model in both Cases. In Case 1, where elasticities are fixed, this variable overwhelmingly dominates, contributing 74% of the total uncertainty. Second order interactions between independent variables play little to no role in driving uncertainty in Case 1. The attribution of uncertainty amongst parameters notably changes when elasticities of demand are included in the analysis. In Case 2, the dominance of income growth is still visible, with 40% of the variance in model output attributed to this variable, however the regression coefficients of price and the covariate coefficient of price x income also play a significant role (contributing more than 10% of the total uncertainty each). It is worth pausing to recall that, as shown in equations (1), (4) and (5), income growth not only drives the governing equation of residential demand (eq. 1) for SFR and MFR sectors, but also plays an important role in the price elasticity of demand. In the case where incomes rise at a rate slower than inflation (in the elasticity equations (4 and 5), income in every year is expressed in 2000 real terms), then this will lead to a less elastic response with regards to income, and a more elastic response with regards to changes in price, and vice versa. The same can be said of the relationship between price and the values of income elasticity.

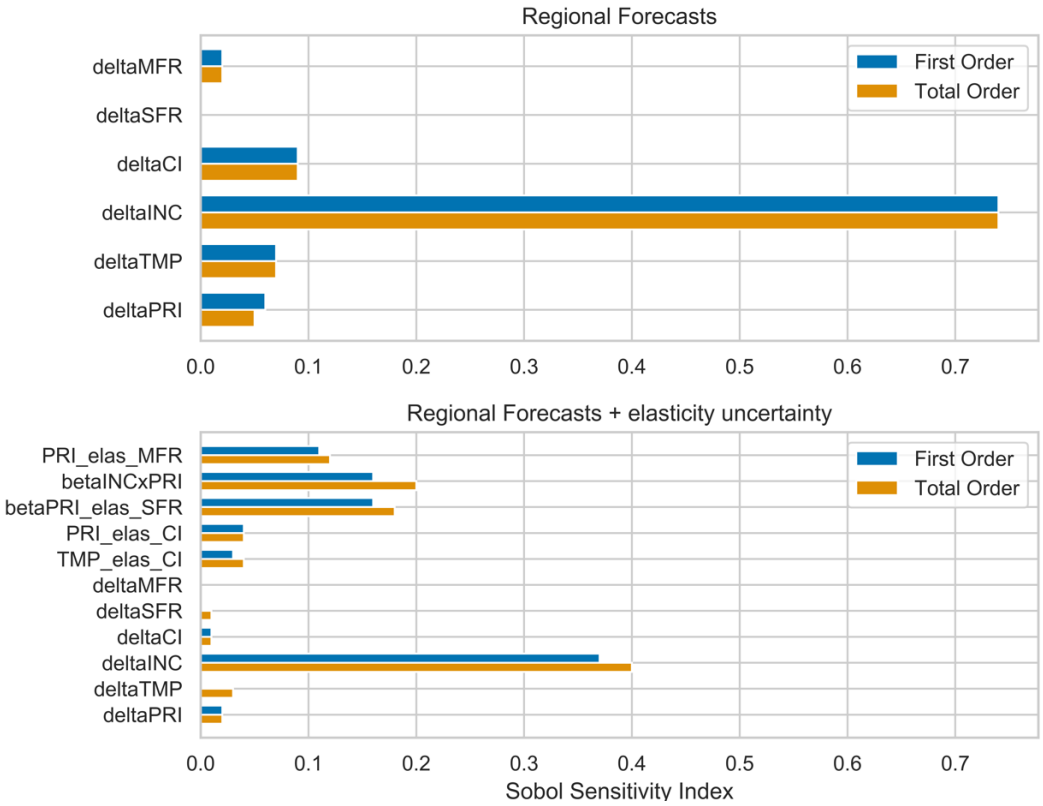

Figure 3-8: First and total order sensitivity indices of uncertain variables sampled across for Case 1 (top) and Case 2 (bottom). Note: only independent variables that had a first order or total order value of >0.015 were included in the above figures

3.3. Findings

Through analysis in this step, we have sought to answer three questions; 1) what is the envelope of uncertainty surrounding the econometric model of demand we are using for long term planning purposes? 2) to which parameters is the model most sensitive to? And 3) what conditions, if any, lead total demand in 2070 in the top 75th percentile of all samples. We employed methodologies from the decision making under deep uncertainty literature to generate many thousands of realizations of demand at the annual time step from 2070, undertook scenario discovery analysis through the use of PRIM, performed linear regression and Sobol sensitivity analysis to understand the sensitivity of the model to its input variables.

We have demonstrated that the envelope of uncertainty associated with demand forecasting is significant under both Cases considered here, and much larger than key examples presented from the literature when the uncertainty associated with elasticity of demand estimates are accounted for. Although the range of scenarios captured by Rayej, et al. (2014) is comparable to the range of demand found for Case 1 where elasticity values are fixed, Bureau of Reclamation. (2012) captured a much smaller range using a similar scenario-based approach. This highlights the dependence of a scenario led approach on the judgement of the decision makers and analysts involved. In some cases a scenario approach may indeed capture the full envelope of uncertainty, however there is no way of knowing if this is the case without quantitative assessment of the uncertainty associated with the demand model in use. It should be noted that the 'Government & Other' sector, representing 20% of total demand across the SFPUC service area was not included in the uncertainty analysis and thus the range of demand produced through this analysis is likely to underestimate the uncertainty.

Scenario discovery reveals a relatively clear answer with regards to those scenarios that lead to policy failure, i.e. demand in the top 25th percentile of all model runs. Income and to a lesser extent price, appear to dominate high demand scenarios in both cases. However, it is challenging to unpack the relative importance of income as a driver of demand in Equation 1 (in combination with income elasticity of demand) vs its role in driving the price elasticity of demand in Equation 5. The low density values for boxes in Case 2, and the shallow nature of the density vs coverage tradeoff curve in Case 2 indicate that these variables cannot necessarily serve as robust predictors of problematic scenarios of demand. Principal Component Analysis as proposed by Dalal et al. (2013) as a preprocessing step to PRIM shows promising results in terms of clustering parameters but does present issues of interpretability.

Sensitivity analysis has revealed the central role that income and price elasticity play in driving the uncertainty in demand projections for SFPUC customers. However, it should be noted that the values for income and price regression coefficients are notably higher than in other comparable studies in the region. Further work should be directed towards better understanding the response of SFPUC customers to price and income, as well as the most likely future projection of income growth for the region in order to reduce the uncertainty they drive in the model.

4. Demand Scenarios for the Stress Test

When extrapolated out to 2070, the 2040 Brattle Group's forecast of demand represents a 45% increase in total demand relative to the Baseline demand for this study – from 305 mgd to 444 mgd (presented in Table 4-2). In order to stress test SFPUC's system against a comprehensive range of plausible futures, a range of demand scenarios must be is established that represent a reasonable envelope of uncertainty for demand SFPUC faces in this regard. The uncertainty analysis (section 3) described in section 3 provides a quantitative basis for doing so. For this study, we consider the 25th exceedance percentile for Case 2 (see Figure 3-3) - 'Regional Forecasts +and elasticity uncertainty' - to represent our upper bound for total demand at 620 million gallons per day (mgd). This value represents a 103% increase in total demand by 2070 relative to our baseline of 305 mgd (see Table 4-2). Given the recent observed negative trend in water sales (see Figure 1-6), and the potential vulnerability a decrease in demand may present (for example with regards to the finance module), we also include a scenario in which demand on the SFPUC system decreases over time. Demand scenarios are placed at 15% intervals between a 'Low' demand scenario (260 mgd) - representing a 15% decrease in total demand - and a 'High' demand scenario (625 mgd) - representing a 105% increase in total demand by 2070 (see Table 4-2).

The 'annual escalation' represents demand growth per year amongst SFPUC's customers when considering the linear trend between Brattle 2010 total demand and that Brattle 2040 total demand (Brattle, 2010, 2014). In the case of Hayward, total demand is projected to decrease by 2040 at a rate of 0.05 mgd/ year. In developing our scenarios of demand, we preserve the spatial variation in demand growth present in the Brattle forecast in all scenarios by applying a multiplier to the 'annual escalation' value. For example, to obtain a 60% increase in total demand relative to the baseline ('Demand 60'), the annual escalation value for each customer is multiplied by a factor of 1.10. The scaling factors and resulting total demand under each scenario are provided in Table 9.

Suburban retail customers were not included in the analysis by Brattle (2018) and so demand forecasts for these customers does not currently exist. We consider suburban retail demand to remain constant in all demand scenarios according to their Baseline value provided in Table 2-1.

The final step in developing scenarios is to establish the SFPUC share of total demand. We use the observed share of total demand for FY2013 to do this and values are provided in Table 4-3. FY2013 can be used as a benchmark for 'normal' conditions prior to the 2013-17 drought. The SFPUC share of total demand under each demand scenario, for each customer is provided in Table 4-3.

Table 4-1: Projection of total demand 2040 (Brattle, 2018) and annual escalation rate based on linear trend from normalized 2010 to year 2040 total demand

CUSTOMER	Annual Escalation (mgd/year)	Normalized total demand in 2010 (mgd)	Brattle Demand in 2040 (AF/d)
Alameda County WD	0.07	45.58	47.76
Brisbane/GVMID	0.00	0.61	0.74
Burlingame	0.02	4.66	5.40
CWS - Bear Gulch	0.06	12.39	14.15
CWS - Mid Peninsula	0.13	15.32	19.19
CWS - South San Francisco	0.06	8.58	10.40
Coastside County WD	0.05	2.03	3.45
Daly City	0.06	6.85	8.66
East Palo Alto WD	0.01	1.81	2.18
Estero MID	0.01	4.72	4.98
Hayward	-0.05	18.08	16.56
Hillsborough	0.03	3.30	4.23
Menlo Park	0.00	3.11	3.20
Mid-Peninsula	0.01	3.09	3.48
Millbrae	0.03	2.40	3.21
Milpitas	0.17	10.68	15.81
Mountain View	0.08	10.49	12.76
North Coast County WD	0.05	3.61	5.12
Palo Alto	0.10	12.26	15.39
Purissima Hills WD	0.02	1.89	2.57
Redwood City	0.04	10.30	11.64
San Bruno	0.03	3.85	4.70
Santa Clara	0.40	4.89	16.76
San Jose	0.20	22.55	28.48
Stanford University	0.06	3.27	5.18
Sunnyvale	0.12	19.83	23.33
Westborough WD	0.00	0.92	1.04
San Francisco	0.31	77.76	87.08
TOTAL	**2.09**	**314.82**	**377.45**

Table 4-2:Total demand scenarios for the stress test

Scenario name	Change from Baseline	Scaling factor*	Total demand mgd
Demand_-15	-15%	0.57	260.28
Base	0%	-	305.49
Demand_15	15%	0.78	350.78
Demand_30	30%	0.89	397.49
Demand_45	45%	1.00	444.20
Demand_60	60%	1.10	487.99
Demand_75	75%	1.21	534.69
Demand_90	90%	1.32	581.40
Demand_105	105%	1.43	625.19

*** Scaling factor applied to annual demand escalation for customers included in Brattle (2018) study. Suburban retail demand remains constant in all scenarios.**

Table 4-3: Total demand and SFPUC's share of total demand per customer for seven of the nine demand scenarios presented here. All values are in million gallons per day (mgd)

CUSTOMER	Share (-)	Demand -15		Baseline		Demand 15		Demand 30		Demand 45		Demand 60		Demand 75	
		Total	SFPUC	Total	SFPUC	Total	SFPUC	Total	SFPUC	Total	SFPUC	Total	SFPUC	Total	SFPUC
Alameda County WD	0.21	28.16	5.91	43.17	9.06	38.80	8.15	44.30	9.30	49.79	10.46	54.94	11.54	60.44	12.69
Brisbane/GVMID	1.00	0.49	0.49	0.32	0.32	0.67	0.67	0.77	0.77	0.86	0.86	0.95	0.95	1.05	1.05
Burlingame	0.93	3.46	3.22	4.48	4.16	4.77	4.44	5.45	5.07	6.12	5.70	6.76	6.29	7.43	6.91
CWS - Bear Gulch	0.95	8.97	8.52	12.71	12.08	12.36	11.74	14.11	13.40	15.86	15.07	17.50	16.62	19.25	18.29
CWS - Mid Peninsula	1.00	13.00	13.00	14.04	14.04	17.91	17.91	20.45	20.45	22.98	22.98	25.36	25.36	27.90	27.90
CWS - South San Francisco	0.93	6.89	6.41	7.41	6.89	9.49	8.83	10.84	10.08	12.18	11.33	13.44	12.50	14.79	13.75
Coastside County WD	0.89	2.75	2.45	1.88	1.67	3.79	3.38	4.33	3.85	4.87	4.33	5.37	4.78	5.91	5.26
Daly City	0.56	5.91	3.31	7.38	4.13	8.15	4.56	9.30	5.21	10.45	5.85	11.53	6.46	12.69	7.10
East Palo Alto WD	1.00	1.44	1.44	2.08	2.08	1.98	1.98	2.26	2.26	2.54	2.54	2.81	2.81	3.09	3.09
Estero MID	1.00	2.96	2.96	4.05	4.05	4.07	4.07	4.65	4.65	5.23	5.23	5.77	5.77	6.35	6.35
Hayward	1.00	8.48	8.48	15.48	15.48	11.68	11.68	13.34	13.34	14.99	14.99	16.54	16.54	18.19	18.19
Hillsborough	1.00	2.91	2.91	3.25	3.25	4.01	4.01	4.58	4.58	5.14	5.14	5.68	5.68	6.24	6.24
Menlo Park	1.00	1.85	1.85	3.24	3.24	2.55	2.55	2.91	2.91	3.27	3.27	3.61	3.61	3.97	3.97
Mid-Peninsula	1.00	2.19	2.19	3.00	3.00	3.01	3.01	3.44	3.44	3.87	3.87	4.27	4.27	4.69	4.69
Millbrae	0.99	2.26	2.24	2.30	2.28	3.12	3.09	3.56	3.53	4.00	3.96	4.42	4.37	4.86	4.81
Milpitas	0.65	11.81	7.68	10.21	6.63	16.28	10.58	18.58	12.08	20.89	13.58	23.05	14.98	25.35	16.48
Mountain View	0.84	8.47	7.12	10.83	9.09	11.68	9.81	13.33	11.20	14.98	12.59	16.53	13.89	18.19	15.28
North Coast County WD	1.00	3.74	3.74	2.51	2.51	5.16	5.16	5.89	5.89	6.62	6.62	7.30	7.30	8.03	8.03
Palo Alto	0.96	10.44	10.02	11.80	11.33	14.39	13.81	16.42	15.77	18.46	17.72	20.37	19.56	22.41	21.51
Purissima Hills WD	1.00	1.83	1.83	1.99	1.99	2.52	2.52	2.88	2.88	3.24	3.24	3.58	3.58	3.93	3.93
Redwood City	0.94	7.32	6.88	9.90	9.31	10.09	9.48	11.51	10.82	12.94	12.17	14.28	13.43	15.71	14.77
San Bruno	0.54	3.14	1.69	3.73	2.01	4.32	2.33	4.93	2.66	5.54	2.99	6.12	3.30	6.73	3.63
Santa Clara	0.10	19.41	1.94	21.77	2.18	26.74	2.67	30.53	3.05	34.32	3.43	37.87	3.79	41.66	4.17
San Jose	0.92	16.14	14.85	4.89	4.50	22.24	20.46	25.39	23.36	28.54	26.26	31.49	28.97	34.64	31.87
Stanford University	0.63	4.00	2.52	3.39	2.14	5.51	3.47	6.29	3.96	7.07	4.45	7.80	4.91	8.58	5.40
Sunnyvale	0.48	15.13	7.26	19.87	9.54	20.86	10.01	23.81	11.43	26.76	12.85	29.53	14.18	32.48	15.59
Westborough WD	1.00	0.65	0.65	0.91	0.91	0.90	0.90	1.02	1.02	1.15	1.15	1.27	1.27	1.39	1.39
San Francisco	1.00	45.59	45.59	58.00	58.00	62.82	62.82	71.71	71.71	80.61	80.61	88.95	88.95	97.84	97.84

5. Shaping demand under seasonal fluctuations in temperature

5.1. Annual base and seasonal demand

In their review of approaches to modelling the response of water demand to changes in climate and weather, Kiefer et al. (2013) established that the approach provided by Maidment and Miaou (1986) provides greater flexibility in defining the effects of seasonality relative to other approaches, and thus was chosen by SFPUC as the approach for this work. The approach relies on decomposing observed water use into base and seasonal components (see Figure 1-3) which represents the proportion that is insensitive to changes in temperature, the base fraction, and that which is sensitive to changes in temperature, the seasonal fraction. This base fraction is generally considered to represent essential uses such as for drinking water, washing, toilet flushing etc., whilst the seasonal portion generally represents non-essential uses such as for watering gardens, washing cars etc. Observed fluctuations in the seasonal component of demand are related to observed maximum temperature in the same timestep to establish a demand-temperature response function – referred to here as the Heat Function.

To establish the base and seasonal components of demand for each customer, SFPUC examined monthly sales data from 2005 – 2017. For each customer, the lowest value of sale volume for the months from December through April is divided by total annual sale volume to estimate the base-over-total demand ratio. The ratios can vary from year to year for customers with multiple sources of supply, in particular in dry years. For this study, it was decided to keep this ratio constant and to set it to its value in FY 2012-2013. As demonstrated in Figure 5-1, the range of base-over-total demand ratio across customers is significant, with a low of 0.31 for Hillsborough, a high of 0.92 for the city of San Francisco and a median value of 0.632. A low ratio indicates a high seasonal component of demand. These differences reflect differences in water use across regions. The base-over-total demand ratio for densely population urban areas such as the city of San Francisco is high, where consumers are less likely to have outdoor space and water use is focused on essential uses.

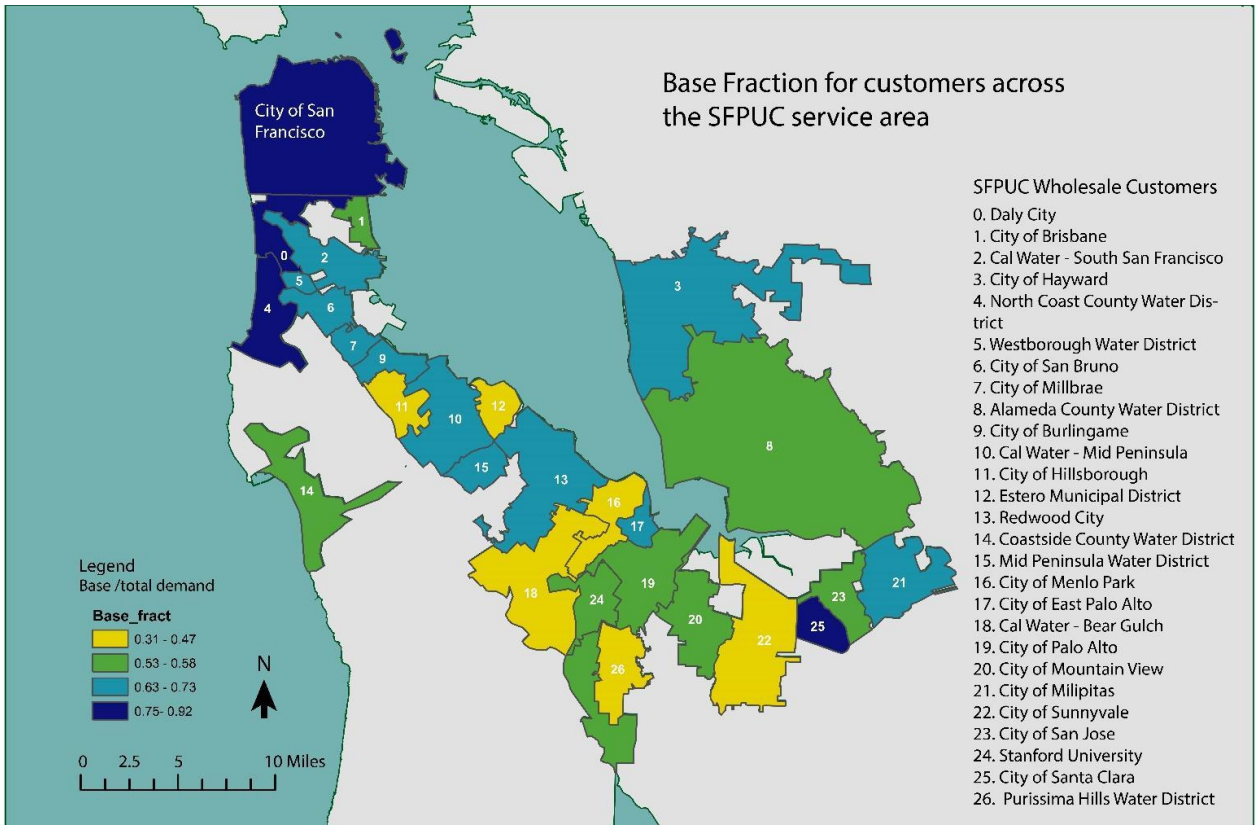

Figure 5-1: Base-over-total demand fraction values across the SFPUC service area for FY2012-2013 which serves as a baseline for the LTVA stress test analysis.

5.2. Heat function

Using a different dataset of weekly deliveries, SFPUC established three heat functions, one for each delivery center (South and East Bay, Peninsula and the City of San Francisco). The heat functions are shown in Figure 5-2 and represent the seasonal response of customers to changes in temperature. To create this heat function, data points have been normalized by the average value of delivery for their corresponding week. This is required to ensure the output of the heat function is a unit-less coefficient that can be applied to the disaggregated, seasonal portion of annual demand. The linear equation that describes the heat function provided in Figure 5-2 is applied to realizations of daily maximum temperature to establish a daily time series of 'Heat Function Factor' that can be applied to the corresponding seasonal component of demand in each time step. To ensure applicability of the Heat function equations to all customers in multiple demand scenarios in the System Model, we added thresholds to avoid negative seasonal demand. In this case between 56°F and 59°F (see heat functions in Figure 5-2) depending on the delivery center. For days in which daily maximum temperature falls below this threshold, the seasonal component of demand is assumed to be zero. The heat function (H_i) for each i delivery center is provided as a function of daily max temperature at San Jose ($tmax_{SJ}$) and San Francisco Airport ($tmax_{SFO}$) gauges in equations 11 through 13.

South and East Bay ($R^2 = 0.75$):

$$H_{SEB} = 0.12tmax_{SJ} - 0.07tmax_{SFO} - 3.03 \quad (11)$$

Peninsula ($R^2 = 0.71$):

$$H_{PEN} = 0.10tmax_{SJ} - 0.05tmax_{SFO} - 3.26 \quad (12)$$

City of San Francisco ($R^2 = 0.65$):

$$H_{CCSF} = 0.07tmax_{SJ} - 3.74 \quad (13)$$

Table 5-1: Table detailing the region in which each customer falls – South and East Bay (SEB), Peninsula (PEN) and CCSF (City of San Francisco)

Customer	Region
Alameda County Water District	SEB
Brisbane/GVMID	PEN
Burlingame	PEN
CWS - Bear Gulch	SEB
CWS - Mid Peninsula	PEN
CWS - South San Francisco	PEN
Coastside County Water District	PEN
Daly City	PEN
East Palo Alto Water District	SEB
Estero MID	PEN
Hayward	SEB
Hillsborough	PEN
Menlo Park	SEB
Mid-Peninsula	PEN
Millbrae	PEN
Milpitas	SEB
Mountain View	SEB
North Coast County Water District	PEN
Palo Alto	SEB
Purissima Hills Water District	SEB
Redwood City	SEB
San Bruno	PEN
Santa Clara	SEB
San Jose	SEB
Stanford University	SEB
City of Sunnyvale	SEB
Westborough Water District	PEN
Cordilleras MWC	CCSF
San Francisco	CCSF

A key assumption in the development and use of these Heat Functions is that delivery is a good proxy for total demand. This is certainly true for all customers relying solely on SFPUC as their source of supply but this may not always hold for customers with multiple sources of supply. As discussed above, in the case of wholesale customers, deliveries only represent the SFPUC share of total demand, thus this assumption may exaggerate the seasonality of demand in the case where the SFPUC share of total wholesale demand in low. Figure 5-2 presents a slice of the heat 'Heat Function Factor' time series for one of the no temperature change climate realizations in which the seasonal shape sought through this analysis is clearly observed.

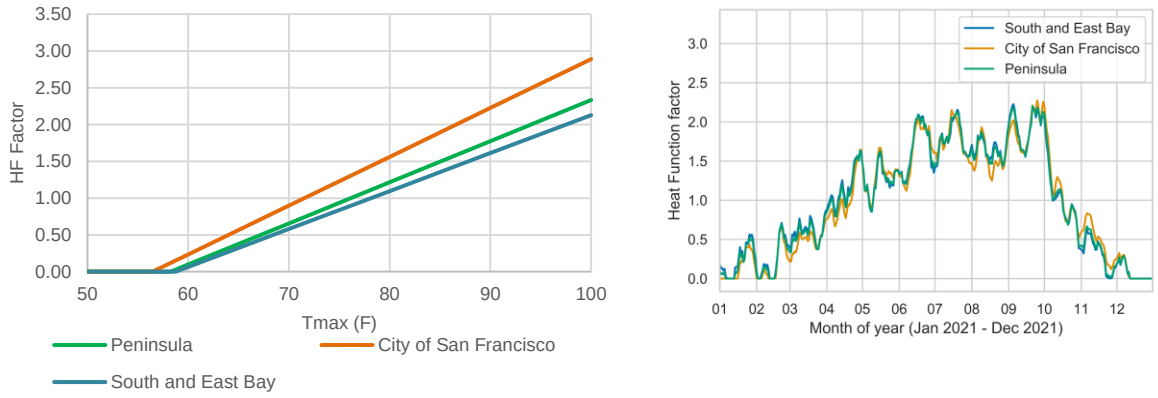

Figure 5-2: Heat functions for the 3 delivery centers (left), and a slice of heat function factor for delivery centers (right)

5.2.1. Post-processing Weather Generator outputs for use in heat-functions

Figure 5-3 shows the SFPUC service area, the area covered by the weather generator, and the location of the San Jose (SJ) and San Francisco Airport (SFO) temperature gauges, which are the gauges of interest for modelling seasonal demand.

As detailed in HRG TR1 (2018), nine stochastic realizations of temperature were generated for the areas covering the three hydrological basins upon which the RWS relies. The relevant spatial domain for demand modeling is shown in Figure 5-3. While the weather generator outputs temperature data at the grid cell level (shaded area in Figure 5-3), the heat functions illustrated in Figure 5-2 use station data for modeling seasonal demand. For this reason, the temperature at the SJ and SFO gauges are estimated from the nearest available grid cell. For SFO, this grid cell is the one in which the SFO gauge lies; and for SJ gauge, that which is located outside the spatial domain included in the weather generator, this grid cell is located east from its location (i.e., grid cells bordered by the red dashed lines in Figure 5-3).

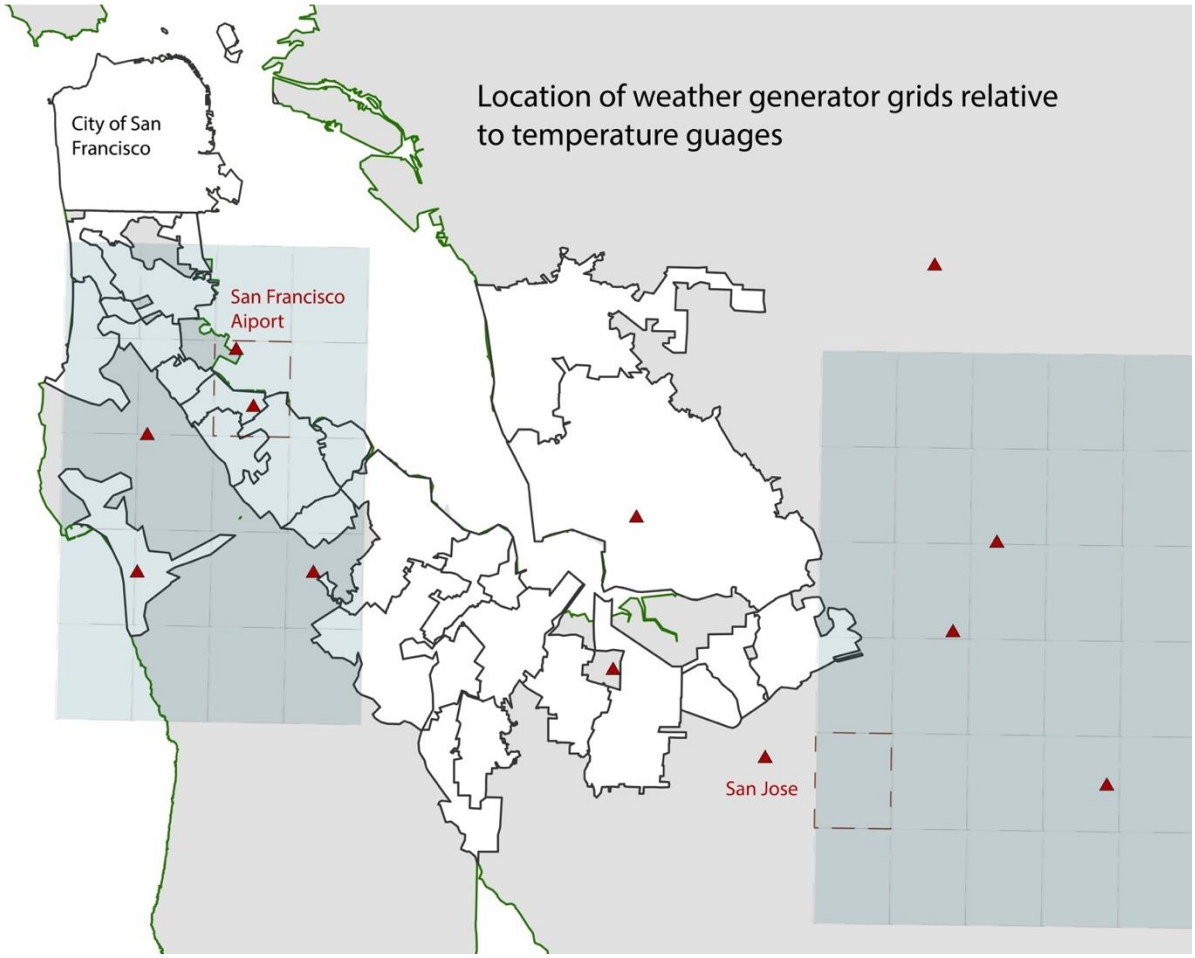

Figure 5-3. Map showing the SFPUC service area. The location of grid cells where the weather generator generates temperature data for South and East Bay and Peninsula regions (shaded areas). Red triangles indicate the location of temperature gauges across the region. San Francisco Airport and San Jose gauges are those used in the development of Heat Functions that are used to scale daily seasonal demand based on daily maximum temperature. The two grid cells bordered with a red dashed line are those used to establish stochastic realizations of climate from the weather generator.

The linear regressions illustrated in Figure 5-4 were developed to estimate the maximum daily temperature at SJ and SFO from the maximum daily temperature at the above-mentioned grid cells and obtained from the stochastic weather generator. However, application of these linear regressions does not allow for a good reproduction of the observed distribution at SFO and SJ, as shown in Figure 5-5. A quantile mapping correction was used to correct the identified bias. Figure 5-5 demonstrates that although the distribution of the corrected simulated temperature although (orange lines) is significantly closer to the observed one, the fit with the distribution of the observed temperature at the gauge is not perfect.

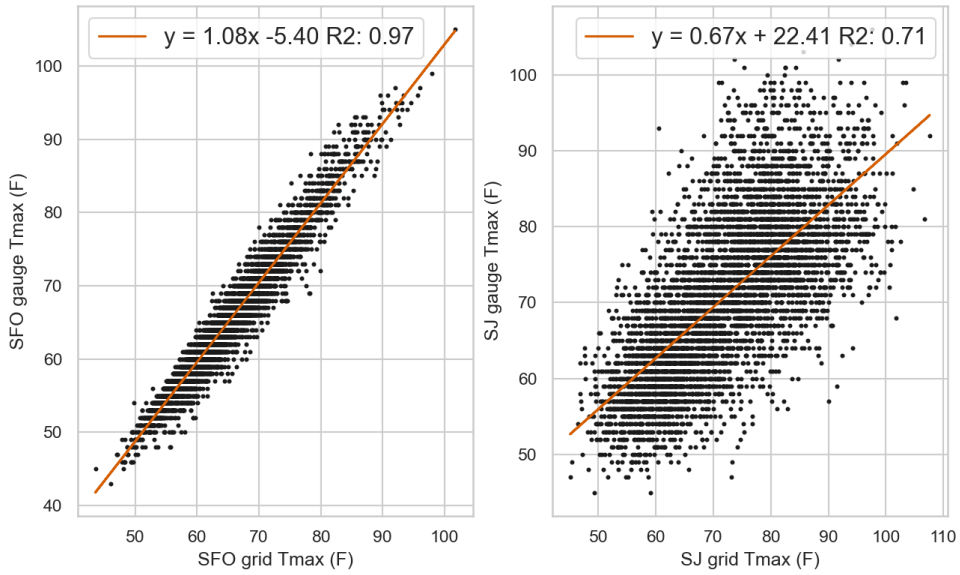

Figure 5-4. Linear regression showing the relationship between the historical temperature at SFO and SJ temperature gauges vs historical temperature for the nearest grid cell.

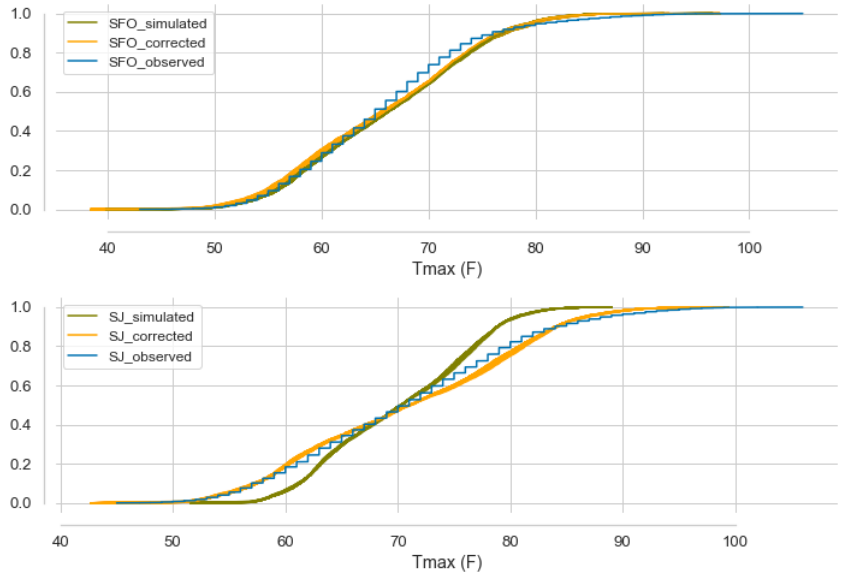

Figure 5-5. Comparison of the cumulative distribution functions obtained from the observed record at the gauge station (blue), the simulated temperature at the gauge using the weather generator output from the nearest grid cell and the linear regression shown in Figure 5-4 (green) and the bias corrected simulated temperature (orange). The top and bottom panels show the distributions for SFO and SJ gauge locations, respectively.

This bias propagates through into the application of the heat functions that shape the seasonal portion of demand and ultimately into average daily demand that is fed into SFWSM. For example, the demand 227mgd demand scenario is in fact 225mgd on average. This bias is outlined in Table

5-2 which provides for each demand scenario the simulated daily average base, seasonal and total demand together with the error.

Table 5-2. Description of the bias in the demand scenarios. The average bias across the 10 realizations from the weather generator is shown. The variability across the stochastic realizations is not significant (standard deviation of the error across the 9 realizations is 0.02mgd, 0.03mgd, 0.03mgd and 0.04mgd, respectively for the demand scenarios 227mgd, 265mgd, 300mgd and 334mgd.

Demand Scenario for the RWS				Simulated Demand for the RWS after daily disaggregation via the heat functions			Model Error	
Name	Base Demand	Seasonal Demand	Total Demand	Simulated Base	Simulated Seasonal	Total	Absolute (mgd)	Relative (%)
227 mgd	157.37	69.42	226.79	157.37	67.84	225.21	-1.57	-0.69
265 mgd	181.61	83.40	265.01	181.61	81.43	263.04	-1.97	-0.74
300 mgd	204.78	94.80	299.58	204.78	92.56	297.34	-2.24	-0.75
334 mgd	227.96	106.18	334.14	227.96	103.68	331.64	-2.50	-0.75

5.3. Long term effects of climate change on demand

The LTVA is concerned with understanding what the impact of climate change will be SFPUC's water system. In order to stress test the system against possible future changes in temperature as a result of climate change, 6 scenarios of temperature increase are used – 0 to 5°C in 1°C intervals. However, little investigation has been directed towards understanding the potential impact of climate change on demand on an inter annual basis:

> *"Relatively few cases are found in the literature where the focus of water modelling on measuring the influence of climate and weather. Even fewer cases have considered how the prospects of climate change may affect water use, and none have studied, at least in any direct sense, whether such prospects might influence choices about modelling methods. (Kiefer et al. 2013)"*

If one applies the heat functions provided in Figure 18 to temperature time series that include scenarios of increasing temperature as a result of climate change then we do not see a change in the seasonality of demand through time but instead see a step change increase in demand. As shown in Figure 19, if we apply a 5 °C increase in temperature to the step change scenarios and then apply the heat functions to shape the seasonal portion of demand, we see a 15% increase in average annual demand relative to the no change scenario. This effect can also be seen in Trend model runs (Figure 19). This is due to the fact that there are very few days in the year in which there is not a seasonal component to demand (i.e. where temperature is below the threshold shown in Figure 18). This is a known shortcoming of the base – seasonal approach to decomposing demand. Climates that can support year-round vegetation growth and irrigation of outdoor

vegetation are likely to capture some climate and weather sensitive elements in the base component of their demand (Kiefer et al., 2013).

If we instead consider the elasticities of demand to temperature established by the Brattle Group (2018), a 5 °C increase (equivalent to 9°F) in temperature, representing a 13% increase in maximum daily temperature (relative to the historical average of 62.28 °F), results in an increase in demand of 6.2% and 1.4% for CI and SFR sectors respectively[3]. This is significantly less than would be implied by using the heat functions as described above.

It seems that for the case of San Francisco, the use of heat functions on temperature timeseries that include climate change likely overstates the role that temperature has in driving demand on an inter annual basis. Particularly when compared to the demand response implied by the temperature elasticities of demand established by Brattle (2018). For this study, we do not link our demand scenarios to a specific scenario of temperature increase but instead use the same base 9 realizations of temperature to shape seasonal intra annual fluctuations in demand for all climate change scenarios.

The question of the impact of climate change on water demand, and the appropriate model to account for such impacts remains an open research question. Energy demand has received comparatively more attention in this regard (Franco and Sanstad, 2008; Thatcher, 2007; Sullivan et al. 2015) and there is likely much we can learn from this sector moving forward.

[3] The elasticities of demand for temperature derived by the Brattle Group (2018) are 0.482 for CI and 0.109 for SFR

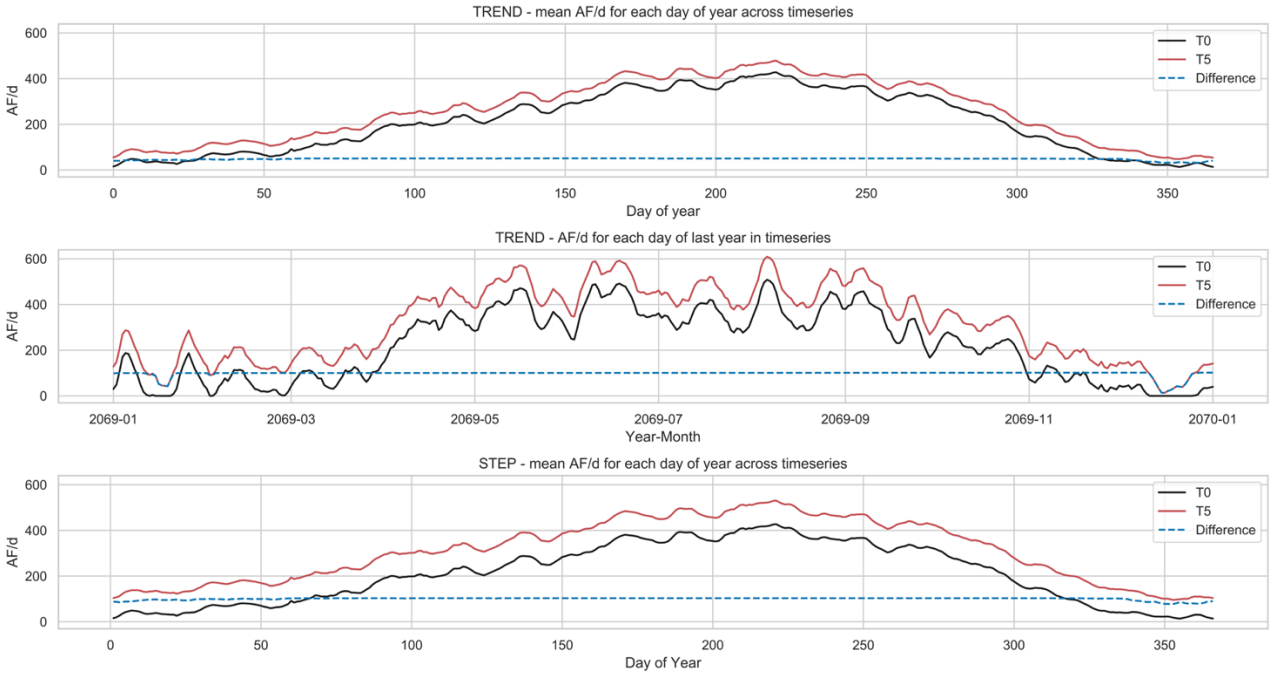

Figure 5-6: illustration of the effect of applying heat functions to timeseries of temperature in which potential changes in climate have been accounted for. Black lines indicate demand in a no temperature change scenario, red lines indicate demand in a +5℃ scenario and dashed blue lines indicate the difference between these two scenarios. Top to bottom: average daily demand for each day of the year across one realization temperature

References

ABAG, 2017. Plan Bay Area 2040: Final Regional Forecast of Jobs, Population and Housing. Association of Bay Area Governments.

Barry, M.E., Coombes, P.J., 2018. Planning resilient water resources and communities: the need for a bottom-up systems approach. Australasian Journal of Water Resources 22, 113–136. https://doi.org/10.1080/13241583.2018.1497125

Billings, R.B., Jones, C.V., 2011. Forecasting Urban Water Demand. American Water Works Association.

Brattle Group, 2018. Socioeconomic Impacts of Water Shortages within the Hetch Hetchy Regional Water System Service Area. Brattle Group.

Brattle Group, 2015. Technical Memorandum: SFPUC Retail Demand Model and Projections through Fiscal Year 2039-40.

Brown, C., Dufour, A., 2017. Long-Term Vulnerability Assessment and Adaptation Planning for the SFPUC Water Enterprise: Technical Memorandum #1 - Identification of Long Term Sources of Vulnerability. University of Massachusetts Amherst.

Brown, C., Ghile, Y., Laverty, M., Li, K., 2012. Decision scaling: Linking bottom-up vulnerability analysis with climate projections in the water sector. Water Resources Research 48. https://doi.org/10.1029/2011WR011212

Bryant, B.P., Lempert, R.J., 2010. Thinking inside the box: A participatory, computer-assisted approach to scenario discovery. Technological Forecasting and Social Change 77, 34–49. https://doi.org/10.1016/j.techfore.2009.08.002

Bureau of Reclamation, 2012. Colorado River Basin Water Supply and Demand Study: Technical Report C: Water Demand Assessment. U.S. Department of the Interior.

Burhenne, S., Jacob, D., Henze, G.P., n.d. Sampling based on Sobol‟ sequences for Monte Carlo techniques applied to building simulations, in: Proceedings of IBPSA BUILDSIM.

CEF, 2017. California County-Level Economic Forecast 2017 - 2050. California Economic Forecast, Santa Barbara.

Chang, H., Parandvash, G.H., Shandas, V., 2010. Spatial Variations of Single-Family Residential Water Consumption in Portland, Oregon. Urban Geography 31, 953–972. https://doi.org/10.2747/0272-3638.31.7.953

Dalal, S., Han, B., Lempert, R., Jaycocks, A., Hackbarth, A., 2013. Improving scenario discovery using orthogonal rotations. Environmental Modelling & Software 48, 49–64. https://doi.org/10.1016/j.envsoft.2013.05.013

Dalhuisen, J.M., Florax, R.J.G.M., Groot, H.L.F. de, Nijkamp, P., 2003. Price and Income Elasticities of Residential Water Demand: A Meta-Analysis. Land Economics 79, 292–308. https://doi.org/10.2307/3146872

Franco, G., Sanstad, A.H., 2008. Climate change and electricity demand in California. Climatic Change 87, 139–151. https://doi.org/10.1007/s10584-007-9364-y

Friedman, J.H., Fisher, N.I., 1999. Bump hunting in high-dimensional data. Statistics and Computing 9, 123–143. https://doi.org/10.1023/A:1008894516817

Fullerton, T.M., Molina, A.L., 2010. Municipal water consumption forecast accuracy. Water Resources Research 46. https://doi.org/10.1029/2009WR008450

Groves, D.G., Bloom, E., 2013. Robust Water-Management Strategies for the California Water Plan Update 2013: Proof-of-Concept Analysis. RAND Corporation, Santa Monica.

Groves, D.G., Bloom, E., Lempert, R.J., Fischbach, J.R., Nevills, J., Goshi, B., 2015. Developing Key Indicators for Adaptive Water Planning. Journal of Water Resources Planning and Management 141, 05014008. https://doi.org/10.1061/(ASCE)WR.1943-5452.0000471

Groves, D.G., Lempert, R.J., 2007. A new analytic method for finding policy-relevant scenarios. Global Environmental Change, Uncertainty and Climate Change Adaptation and Mitigation 17, 73–85. https://doi.org/10.1016/j.gloenvcha.2006.11.006

Haasnoot, M., Kwakkel, J.H., Walker, W.E., ter Maat, J., 2013. Dynamic adaptive policy pathways: A method for crafting robust decisions for a deeply uncertain world. Global Environmental Change 23, 485–498. https://doi.org/10.1016/j.gloenvcha.2012.12.006

Hadka, D., 2017. Platypus: A free and open source python library for multiobjective optimization.

Hallegatte, S.S., Ankur Lempert, Robert Brown, Casey Gill, Stuart, 2012. Investment Decision Making under Deep Uncertainty - Application to Climate Change, Policy Research Working Papers. The World Bank. https://doi.org/10.1596/1813-9450-6193

Hazen & Sawyer, 2012. Tampa Bay Water's Revised Probabilistic Demand Forecasting Procedure and Base-Year 2010 Probabilistic Demand Forecast. Prepared for Tampa Bay Water.

Helton, J.C., Davis, F.J., 2003. Latin hypercube sampling and the propagation of uncertainty in analyses of complex systems. Reliability Engineering & System Safety 81, 23–69. https://doi.org/10.1016/S0951-8320(03)00058-9

Herman, J., Usher, W., 2017. SALib: An open-source Python library for Sensitivity Analysis. The Journal of Open Source Software 2, 97. https://doi.org/10.21105/joss.00097

House-Peters, L.A., Chang, H., 2011. Urban water demand modeling: Review of concepts, methods, and organizing principles. Water Resources Research 47. https://doi.org/10.1029/2010WR009624

Iooss, B., Lemaître, P., 2015. A Review on Global Sensitivity Analysis Methods, in: Dellino, G., Meloni, C. (Eds.), Uncertainty Management in Simulation-Optimization of Complex Systems: Algorithms and Applications, Operations Research/Computer Science Interfaces Series. Springer US, Boston, MA, pp. 101–122. https://doi.org/10.1007/978-1-4899-7547-8_5

Kiefer, J., Dziegielewski, B., Henderson, J., 2013. Changes in Water Use Under Regional Climate Change Scenarios. Water Research Foundation.

Kiefer, J., Yoe, C., Clayton, J., Leonard, J., 2016. Uncertainty in Long-Term Water Demand Forecasts: A Primer on Concepts and Review of Water Industry Practices. Water Research Foundation.

Kwakkel, J.H., 2017. The Exploratory Modeling Workbench: An open source toolkit for exploratory modeling, scenario discovery, and (multi-objective) robust decision making. Environmental Modelling & Software 96, 239–250. https://doi.org/10.1016/j.envsoft.2017.06.054

Kwakkel, J.H., Jaxa-Rozen, M., 2016. Improving scenario discovery for handling heterogeneous uncertainties and multinomial classified outcomes. Environmental Modelling & Software 79, 311–321. https://doi.org/10.1016/j.envsoft.2015.11.020

Lempert, R., Nakicenovic, N., Sarewitz, D., Schlesinger, M., 2004. Characterizing Climate-Change Uncertainties for Decision-Makers. An Editorial Essay. Climatic Change 65, 1–9. https://doi.org/10.1023/B:CLIM.0000037561.75281.b3

Maidment, D.R., Miaou, S.-P., 1986. Daily Water Use in Nine Cities. Water Resources Research 22, 845–851. https://doi.org/10.1029/WR022i006p00845

Maidment, D.R., Miaou, S.-P., Crawford, M.M., 1985. Transfer Function Models of Daily Urban Water Use. Water Resources Research 21, 425–432. https://doi.org/10.1029/WR021i004p00425

Mcculloch, C., n.d. The Kielder Water Scheme: the last of its kind? 15.

McKay, M.D., Beckman, R.J., Conover, W.J., 1979. Comparison of Three Methods for Selecting Values of Input Variables in the Analysis of Output from a Computer Code. Technometrics 21, 239–245. https://doi.org/10.1080/00401706.1979.10489755

Paton, F.L., Maier, H.R., Dandy, G.C., 2013. Relative magnitudes of sources of uncertainty in assessing climate change impacts on water supply security for the southern Adelaide water supply system. Water Resources Research 49, 1643–1667. https://doi.org/10.1002/wrcr.20153

Pitkin, J., Myers, D., 2012. Generational Projections of the California Population By Nativity and Year of Immigrant Arrival.

RAND, n.d. Climate Information Workshop Goals, Process and Results. RAND Corporation.

Rayej, M., Juricich, R., Groves, D., Yates, D., 2014. Scenarios of Future California Water Demand through 2050: Growth and Climate Change. American Society of Civil Engineers, Palm Springs, California, United States.

Rinaudo, J.-D., 2015. Long-Term Water Demand Forecasting, in: Grafton, Q., Daniell, K.A., Nauges, C., Rinaudo, J.-D., Chan, N.W.W. (Eds.), Understanding and Managing Urban Water in Transition, Global Issues in Water Policy. Springer Netherlands, Dordrecht, pp. 239–268. https://doi.org/10.1007/978-94-017-9801-3_11

Saltelli, A. (Ed.), 2008. Global sensitivity analysis: the primer. John Wiley, Chichester, England ; Hoboken, NJ.

Saltelli, A., 2002. Making best use of model evaluations to compute sensitivity indices. Computer Physics Communications 145, 280–297. https://doi.org/10.1016/S0010-4655(02)00280-1

Saltelli, A., Aleksankina, K., Becker, W., Fennell, P., Ferretti, F., Holst, N., Li, S., Wu, Q., 2019. Why so many published sensitivity analyses are false: A systematic review of sensitivity analysis practices. Environmental Modelling & Software 114, 29–39. https://doi.org/10.1016/j.envsoft.2019.01.012

Saltelli, A., Annoni, P., Azzini, I., Campolongo, F., Ratto, M., Tarantola, S., 2010. Variance based sensitivity analysis of model output. Design and estimator for the total sensitivity index. Computer Physics Communications 181, 259–270. https://doi.org/10.1016/j.cpc.2009.09.018

Saltelli, A., Tarantola, S., Chan, K.P.-S., 1999. A Quantitative Model-Independent Method for Global Sensitivity Analysis of Model Output. Technometrics 41, 39–56. https://doi.org/10.1080/00401706.1999.10485594

Sebri, M., 2014. A meta-analysis of residential water demand studies. Environ Dev Sustain 16, 499–520. https://doi.org/10.1007/s10668-013-9490-9

SFPUC, 2018. Water Sales Data 1992-2016 [Unpublished Data].

SFPUC, 2016. 2015 Urban Water Management Plan for the City and County of San Francisco. San Francisco Public Utilities Commission.

SFPUC, 2009. Water Supply Agreement between the City of San Francisco and Wholesale Customers in Alameda County, San Mateo County and Santa Clara County.

Sobol′, I.M., 2001. Global sensitivity indices for nonlinear mathematical models and their Monte Carlo estimates. Mathematics and Computers in Simulation 55, 271–280. https://doi.org/10.1016/S0378-4754(00)00270-6

Sobol', I.M., 1967. On the distribution of points in a cube and the approximate evaluation of integrals. USSR Computational Mathematics and Mathematical Physics 7, 86–112. https://doi.org/10.1016/0041-5553(67)90144-9

Sobol', I.M., Levitan, Yu.L., 1999. A pseudo-random number generator for personal computers. Computers & Mathematics with Applications 37, 33–40. https://doi.org/10.1016/S0898-1221(99)00057-7

Sullivan, P., Colman, J., Kalendra, E., 2015. Predicting the Response of Electricity Load to Climate Change (No. NREL/TP--6A20-64297, 1215283). https://doi.org/10.2172/1215283

Thatcher, M.J., 2007. Modelling changes to electricity demand load duration curves as a consequence of predicted climate change for Australia. Energy 32, 1647–1659. https://doi.org/10.1016/j.energy.2006.12.005

Tiwari, M.K., Adamowski, J., 2013. Urban water demand forecasting and uncertainty assessment using ensemble wavelet-bootstrap-neural network models. Water Resources Research 49, 6486–6507. https://doi.org/10.1002/wrcr.20517

HRG TR4 (2021). Technical Report 4: San Francisco Water System Model. Hydrosystems Research Group, University of Massachusetts, Amherst, Amherst, Massachusetts.

HRG TR1 (2018). Technical Report 1: Weather Generator Module. Hydrosystems Research Group, University of Massachusetts, Amherst, Amherst, Massachusetts.

Walker, G., 2013. A critical examination of models and projections of demand in water utility resource planning in England and Wales. International Journal of Water Resources Development 29, 352–372. https://doi.org/10.1080/07900627.2012.721679

Walker, W.E., Lempert, R.J., Kwakkel, J.H., 2013. Deep Uncertainty, in: Gass, S.I., Fu, M.C. (Eds.), Encyclopedia of Operations Research and Management Science. Springer US, Boston, MA, pp. 395–402. https://doi.org/10.1007/978-1-4419-1153-7_1140

Wentz, E.A., Gober, P., 2007. Determinants of Small-Area Water Consumption for the City of Phoenix, Arizona. Water Resour Manage 21, 1849–1863. https://doi.org/10.1007/s11269-006-9133-0